UNCLASSIFIED

GEMP-19A

AMPTIAC

Nuclear Materials & Propulsion Operation

High-Temperature Materials Program

Progress Report No. 19, Par

JANUARY 25, 1963

FLIGHT PROPULSION LABORATORY DEPARTMENT
GENERAL ⒼⒺ ELECTRIC

	MECHANICAL PROPERTIES DATA CENTER
DATA INPUT RECORD	BY	MO.	DAY	YR.
REFERENCE NO. D77	Fred	10	3	67
ENCODED				
EDITED	P.C.	10	10	67
KEYPUNCHED	VP	10	17	67
VERIFIED	EY	10	18	67
REPRODUCED				
ENC: FORMS FILED				

A-1420-19

High-Temperature Materials Program
Progress Report No. 19, Part A

JANUARY 25, 1963

United States Atomic Energy Commission   Contract No. AT(40-1)-2847

NUCLEAR MATERIALS and PROPULSION OPERATION
FLIGHT PROPULSION LABORATORY DEPARTMENT

GENERAL ELECTRIC

Cincinnati 15, Ohio

DISTRIBUTION

EXTERNAL

AEC Headquarters
- G. M. Anderson
- T. Benson
- I. Hoffman
- T. W. McIntosh
- R. G. Oehl
- F. C. Schwenk
- J. M. Simmons (2)
- W. Tesch
- G. W. Wensch

AEC, OROO
- D. F. Cope (3)
- D. S. Zachry, Jr.

AEC, CAO
- C. L. Karl
- J. F. Weissenberg

AEC, NYOO
- M. Balicki

AEC, SAN
- G. F. Helfrich

AEC, MCR Project Office
- S. Meyers

General Atomic
- G. B. Engle
- W. C. Moore

Pratt and Whitney Aircraft (CANEL)
- L. M. Raring (3)

ORNL
- R. E. Blanco
- R. E. Clausing
- D. A. Douglas, Jr.
- W. R. Grimes
- W. O. Harms
- W. D. Manley
- A. J. Miller
- N. W. Rosenthal

BMI
- R. W. Dayton

LASL
- R. D. Baker

Lawrence Radiation Laboratory
- R. E. Batzel
- C. Cline
- A. J. Rothman

National Bureau of Standards
- H. S. Parker

Atomics International
- S. C. Carniglia

W. R. Grace and Company
- F. T. Fitch

NASA Headquarters
- J. J. Lynch

INTERNAL

- E. A. Aitken
- W. G. Baxter
- J. R. Beeler
- J. C. Blake
- H. C. Brassfield
- R. W. Brisken
- V. P. Calkins
- C. L. Chase (3)
- D. Cochran
- C. G. Collins
- E. S. Collins
- J. F. Collins
- P. K. Conn
- J. B. Conway
- E. B. Delson
- H. S. Edwards
- E. W. Filer

- P. N. Flagella
- J. E. Fox
- E. S. Funston
- M. Goldstein
- G. F. Hamby
- J. O. Hibbits
- A. N. Holden, APED (2)
- L. D. Jordan
- G. Korton
- M. C. Leverett
- W. H. Long
- R. A. Lutter
- L. R. McCreight MSD
- J. A. McGurty
- C. I. McVey
- J. W. Morfitt (2)
- J. Moteff
- R. E. Motsinger
- G. T. Muehlenkamp
- G. Neumann

- C. E. Niemeyer
- W. E. Niemuth
- G. W. Pomeroy
- W. Z. Prickett
- R. C. Rau
- F. C. Robertshaw
- M. T. Schoenberger
- R. J. Spera
- H. R. Stephan
- G. Thornton
- P. P. Turner
- F. O. Urban
- G. R. VanHouten
- H. Wagner
- J. F. White
- D. B. Williams
- O. G. Woike
- R. E. Wood
- Library (10)

2

CONTENTS

FIGURES

TABLES

1. INTRODUCTION AND SUMMARY

Introduction

This report is the unclassified portion of the nineteenth in a series of monthly reports of the work in process on materials development for the Atomic Energy Commission under Contract AT(40-1)-2847.

Included is a summary of the work from October 15, 1962, to December 15, 1962, on three of the fourteen specific development programs in process. Five of the remaining programs are reported in the classified portion of this report, GEMP-19, Part B. The other six, involving the development of ceramic fuel materials, are reported in alternate months.

Summary

HIGH-TEMPERATURE REACTOR MATERIALS FABRICATION RESEARCH (57003)

Stress-rupture results obtained with molybdenum at 2200°C in hydrogen and argon were essentially identical indicating little or no atmosphere effect. Previous data which indicated longer rupture life (and increased creep resistance) in the argon tests have been discounted because of tungsten contamination of the sample material during testing as revealed by chemical analysis.

Identical results at 2200°C in both hydrogen and argon were obtained on two of the three different heats of molybdenum employed in the stress-rupture tests. The third heat exhibited much longer rupture life, particularly at a stress level of 1000 psi. The reason for this difference has not been identified but is probably caused by some material variability.

The stress-rupture properties of tantalum were evaluated in two grades of argon and two grades of hydrogen. The stress-rupture life in argon was found to decrease as the dewpoint was decreased. Tungsten contamination was found on the surface of tantalum samples tested in the "wet" argon due, in all probability, to the transport of tungsten from the furnace heating element by the tungsten-water vapor cycle. This observation stresses the importance of employing extremely low (about -75°C) dewpoints in stress-rupture tests in noble gas atmospheres at elevated (2000°C) temperatures. There was no significant difference noted in the tantalum stress-rupture life test data obtained for tests conducted in commercial (2000 ppm impurities) and high purity grade hydrogen (5 ppm impurities).

EFFECTS OF RADIATION ON HIGH-TEMPERATURE ALLOYS (57004)

The preliminary experimental program on the refractory metals was initiated with the irradiation of several tungsten and molybdenum flat test specimens. Support equipment and furnaces for testing at high temperature in hydrogen or inert atmosphere or in vacuum are being assembled.

All the tensile data generated on A-286, Hastelloy X, and Rene' 41 has now been reported. The effects of irradiation on the stress rupture properties of overaged and underaged specimens of Rene' 41 are presented.

Preliminary studies on the creep-rupture properties of Hastelloy X are illustrated in the form of specimen elongations as a function of testing time for various temperatures and stresses.

Studies on the number of atom displacements in iron due to neutrons of various energies are discussed. The angular distribution of neutron scattering in iron and also the effect of the angle of neutron incidence on the medium are presented. The influence of material geometry on the number of atom displacements per unit flux is demonstrated by comparing the displacements in an iron column with those in an iron slab for various base widths and thicknesses.

LONG TERM IRRADIATION TEST OF 80Ni - 20Cr FUEL ELEMENT SPECIMEN (57301)

No further work was done during this reporting period. A final summary will be included in the 1963 High-Temperature Materials Annual Report.

2. HIGH-TEMPERATURE
REACTOR MATERIALS FABRICATION RESEARCH

(57003)

The purpose of this program is to develop and evaluate methods of preparing and joining refractory metals and alloys, and other high-temperature materials for use as fueled and non-fueled high temperature (1000° to 3000°C) reactor components.

STRESS-RUPTURE TEST RESULTS

Molybdenum

Stress-rupture testing of molybdenum at 2200°C in hydrogen and argon was continued in this reporting period. Previous stress-rupture tests[*][†] were performed by loading the specimen before heating. During this report period, equipment was modified to allow the load to be applied after the specimen reached test temperature. With this technique, an unstressed heat treatment of the specimen can be obtained and the opportunity to obtain first-stage creep data is enhanced. No significant variation from previously reported stress-rupture data has been observed at the temperatures used in tests to date.

The tests performed during this reporting period on the three heats of molybdenum, designated Mo-A, Mo-B, Mo-C, are summarized in Table 2.1. All of the Mo-A, Mo-B, Mo-C stress-rupture results obtained to date are shown in Figures 2.1 and 2.2. These data show that Mo-B (0.011 inch thick) and Mo-C (0.015 inch thick) have equivalent stress-rupture properties at 2200°C in both hydrogen and argon at the stress levels investigated. Mo-A (0.010 inch thick), in argon and hydrogen, exhibits a rupture life, at equivalent loads, which is much longer than that of either Mo-B or Mo-C, particularly at stress levels above 400 psi. However, if the ten-hour stress-rupture levels are extrapolated to 100-hour life, the variation between Mo-A and Mo-B or Mo-C appears to be negligible. The results of chemical analyses of as-received Mo-A, Mo-B, and Mo-C are so similar that strength differences cannot readily be attributed to variations in material composition. Additional studies involving electron microscopy and electron diffraction evaluations are now under way to investigate possible intergranular deposits which might be responsible for these strength differences.

Photomicrographs of "as-received" material are shown in Figure 2.3. While these structures appear identical, a more detailed examination at higher magnification revealed incipient recrystallization in the Mo-A sample but none in Mo-B. Hardness measurements for as-received material were 252 DPH for Mo-A and 275 DPH for Mo-B.

---

[*]"High-Temperature Materials Program Progress Report No. 17, Part A," GE-NMPO, GEMP-17A, November 15, 1962, p. 19.

[†]"High-Temperature Materials Program Progress Report No. 15, Part A," GE-NMPO, GEMP-15A, September 14, 1962, p. 21.

TABLE 2.1

HIGH-TEMPERATURE STRENGTH DATA FOR MOLYBDENUM

| Material	Temperature, °C	Atmosphere	Stress, psi	Time To Effect Indicated Strain, hr				Percent Elongation In 1-Inch Gage Length
				Elongation, %			Rupture	
				2	5	10		
Mo-A	2200	H_2	550	0.4	1.2	2.65	6.70	29.7
Mo-A	2200	H_2	600	0.2	0.8	2.0	6.18	30.9
Mo-A	2200	H_2	700	0.2	0.8	1.6	3.44	26.0
Mo-A	2200	H_2	800	0.2	0.7	1.4	2.83	20.2
Mo-A	2200	H_2	1000	0.2	0.5	1.0	1.69	20.9
Mo-A	2200	A	600	0.5	1.5	3.0	5.75	14.3
Mo-A	2200	A	700	0.4	1.0	2.2	4.30	21.3
Mo-A	2200	A	900	0.2	0.7	1.6	2.75	19.2
Mo-A	2200	A	1100	0.1	0.4	1.0	1.56	17.5
Mo-A	2200	A	1300	0.2	0.4	0.8	1.10	16.0
Mo-B	2200	H_2	400	0.3	1.0	2.0	6.7	50.4
Mo-B	2200	H_2	500	0.1	0.4	1.1	3.22	47.5
Mo-B	2200	H_2	600	0.1	0.3	0.6	1.49	49.5
Mo-B	2200	H_2	700	0.06	0.2	0.4	0.81	58.1
Mo-B	2200	A	400	0.3	0.9	2.0	5.57	37.2
Mo-B	2200	A	500	0.1	0.4	1.0	2.95	59.4
Mo-B	2200	A	600	0.1	0.3	0.5	1.33	54.2
Mo-B	2200	A	700	0.06	0.1	0.3	0.58	30.4
Mo-C	2200	H_2	300	1.1	2.8	5.2	12.05	60.2
Mo-C	2200	H_2	450	0.2	0.7	1.3	2.72	64.0
Mo-C	2200	H_2	550	0.08	0.3	0.5	1.48	90.5
Mo-C	2200	H_2	600	0.07	0.2	0.4	1.28	105.5
Mo-C	2200	H_2	750	0.04	0.1	0.2	0.53	57.2
Mo-C	2400	H_2	400	0.03	0.08	0.2	0.4	61.5
Mo-C	2200	A	300	1.3	2.9	5.2	15.37	70.6
Mo-C	2200	A	450	0.2	0.7	1.4	3.25	47.2
Mo-C	2200	A	550	0.1	0.3	0.7	1.87	103.8
Mo-C	2200	A	700	0.08	0.1	0.2	0.45	78.8
Mo-C	2200	A	900	0.01	0.03	0.07	0.16	79.7
Mo-C	2400	A	400	0.03	0.07	0.2	0.31	66.0
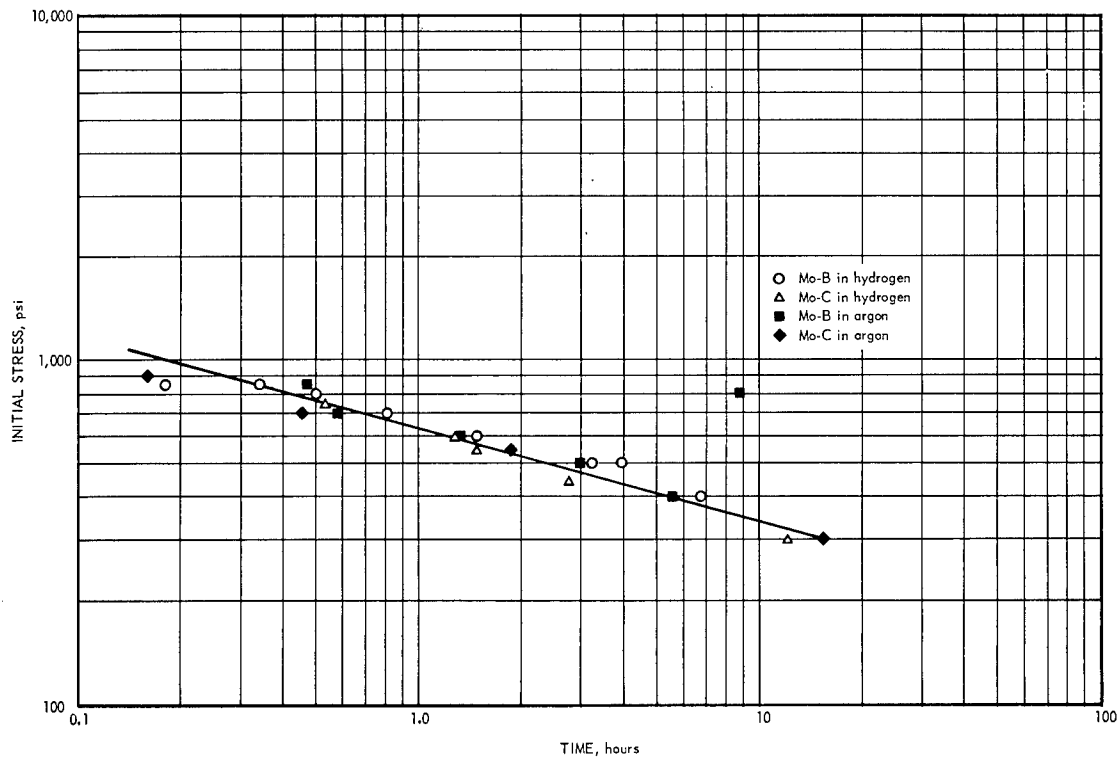
Fig. 2.1—Results of Mo-B and Mo-C stress-rupture tests in hydrogen and argon at 2200°C
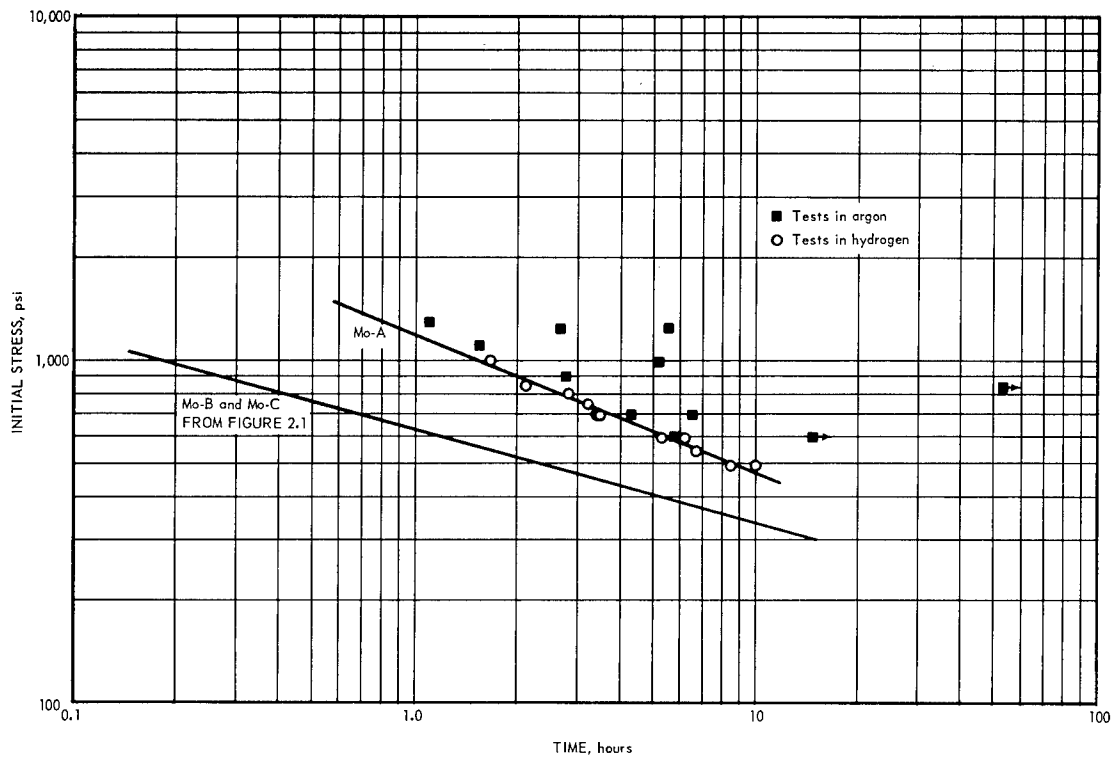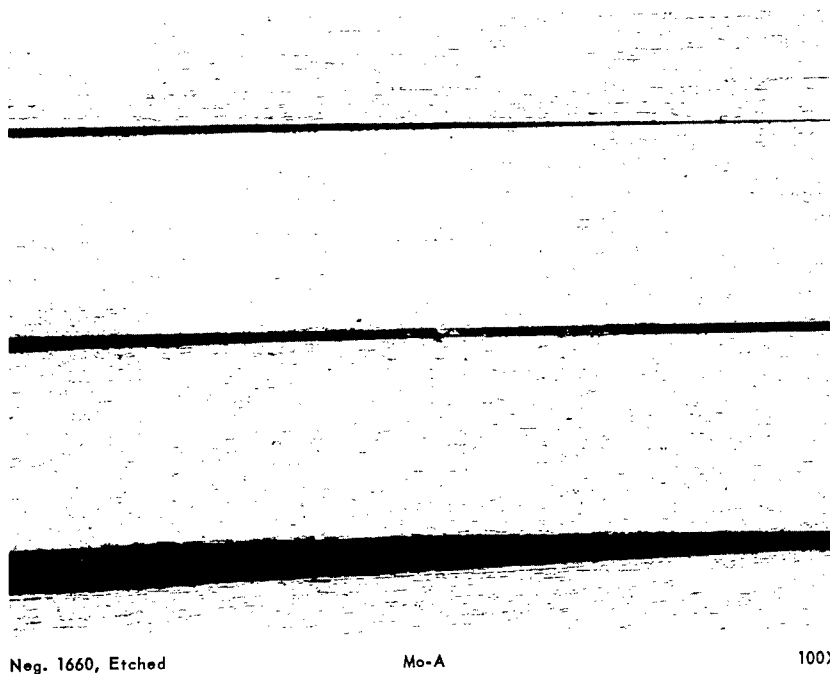

Fig. 2.2—Results of Mo-A stress-rupture tests in hydrogen and argon at 2200°C
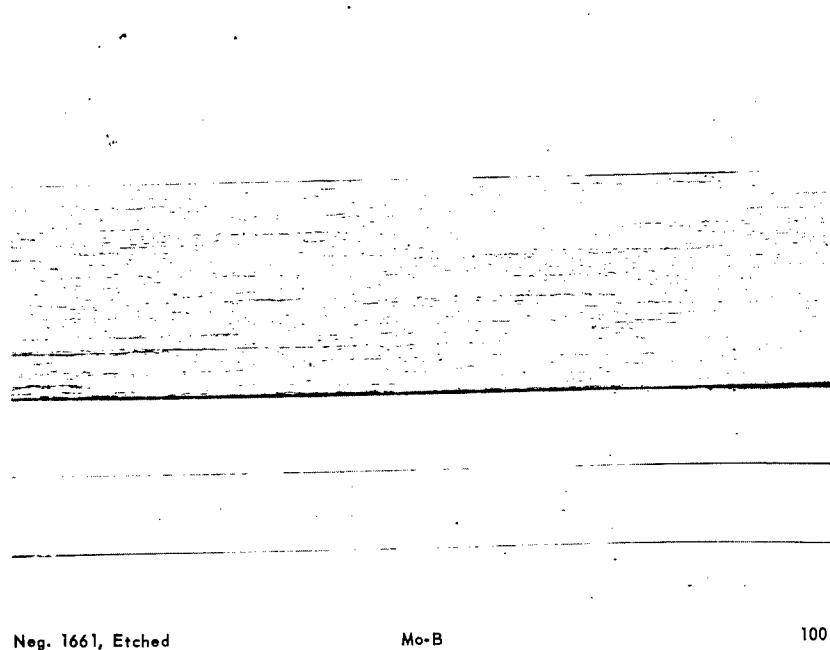
Neg. 1660, Etched   Mo-A   100X

Neg. 1661, Etched   Mo-B   100X

Fig. 2.3 — Photomicrographs of as-received Mo-A and Mo-B
material

Typical microstructures of Mo-A and Mo-B after testing at 2200°C and 500 psi in hydrogen are shown in Figure 2.4. The Mo-A specimen which ruptured after 10 hours at temperature exhibited small uniform and equiaxed grains with grain boundary separation increasing near the fracture. The Mo-B specimen which ruptured after 3.9 hours at temperature exhibited very large and equiaxed grains. This difference in grain size was noticed consistently and may in some way be responsible for the observed difference in strength. Another difference noted involves a higher recrystallization temperature for Mo-B.

Figures 2.5, 2.6, and 2.7 show typical specimens of Mo-A, Mo-B, and Mo-C after test and point out the differences in types of fracture at failure as well as a comparison of the elongations.

Some previous tests of molybdenum in argon produced results which were markedly different from those obtained in hydrogen at the same temperature and stress level. Not only was the rupture life higher, as shown in Figures 2.1 and 2.2, but the creep resistance was observed to be increased by an order of magnitude. Chemical analyses have since revealed that these specimens were contaminated with tungsten which probably accounts for the observed increase in strength. The source of this tungsten is obviously the furnace heating element. Since vapor pressures are too low to account for such transport and no tungsten contamination was found in other specimens heated in the high purity gases normally used to conduct these tests, the contamination must be due to the formation of the volatile tungsten oxide resulting from either the tungsten-water vapor cycle or the reaction of tungsten with air which entered the furnace through defective seals. The fact that this unusual strength is observed only occasionally points to some inadvertent deviation from ordinarily carefully controlled test conditions. Some proof of the contaminating mechanism was obtained when a molybdenum specimen was deliberately coated with a thin film of tungsten oxide and tested in argon. This test showed exactly the same increased strength referred to above. Interestingly, this same test in hydrogen failed to show any property increase. Since in this test the film of tungsten oxide was quickly reduced to a film of tungsten, it seems that the strengthening mechanism must be associated with the presence of a volatile oxide phase. Further tests are planned to more clearly define this phenomenon.

Chemical analysis of three of these Mo(W) specimens showed that the amount of tungsten absorbed was a function of the time the test sample was at temperature. An electron microprobe analysis of one of these samples showed that the concentration of tungsten was high (22%) on the surface and low (1 to 2%) in the center of the material. No tungsten contamination was observed in specimens which exhibited a stress-rupture life falling close to the lines in Figures 2.1 and 2.2. Obviously, the test results in argon are affected only when the furnace atmosphere is inadvertently contaminated with tungsten oxide.

Tantalum

Previous stress-rupture tests of tantalum at 2600°C in argon have shown a certain amount of scatter compared to the fairly reproducible results obtained in the hydrogen tests. In order to determine the effect of various atmospheres on identical tantalum specimens, a series of tests was conducted using two sources of hydrogen and two sources of argon as defined below:

1. Hydrogen from the plant distribution system
2. Bottled high purity hydrogen
3. Argon from the plant distribution system
4. Bottled liquid argon

Table 2.2 presents a summary of these 2600°C tests with a specimen stress of 170 psi.

Neg. 1577, Etched   Mo-A   100X

Neg. 1576, Etched   Mo-B   100X
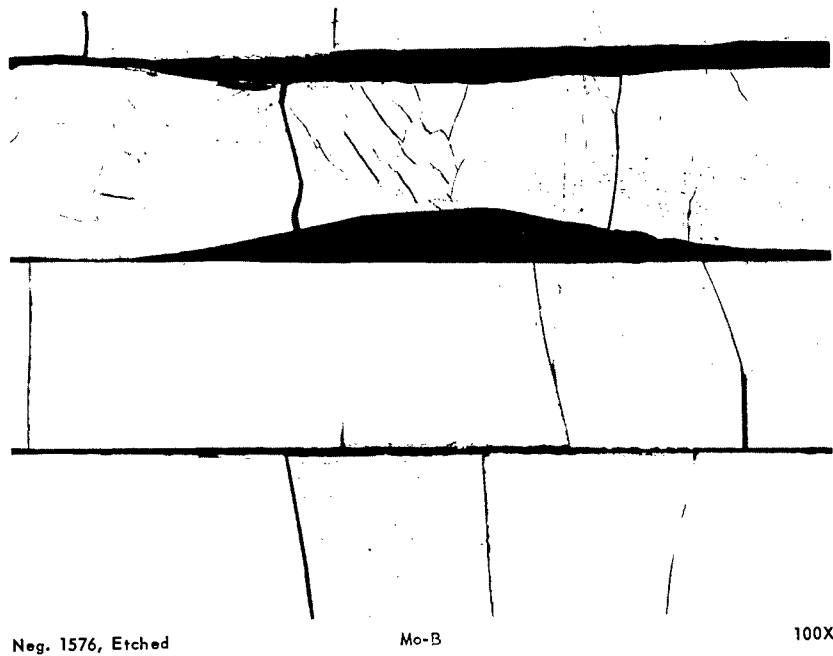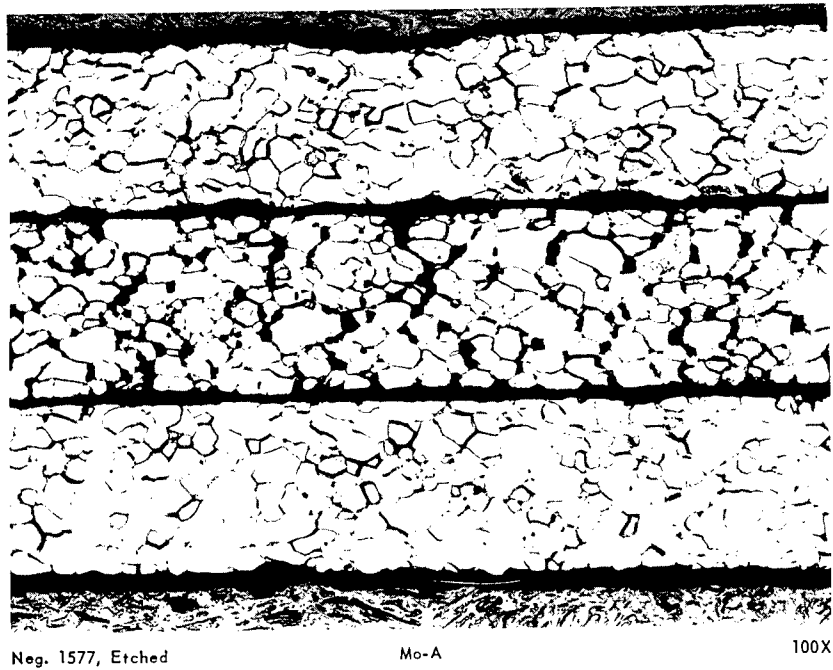
Fig. 2.4 — Photomicrographs of Mo-A and Mo-B tested at
2200°C and 500 psi in H_2 for 10 and 3.9 hours,
respectively

No. 1   No. 2   No. 3   No. 4   No. 5   No. 6   No. 7

INITIAL STRESS, psi

| 600 | 500 | 800 | 1000 | 1300 | 1100 | 900 |

TIME TO RUPTURE, hours

| 6.18 | 6.7 | 2.83 | 1.69 | 1.10 | 1.56 | 2.75 |

PERCENT ELONGATION IN 1-INCH GAUGE LENGTH

| 30.9 | 29.7 | 20.2 | 20.9 | 16.0 | 17.5 | 19.2 |

TEST ATMOSPHERE

| Hydrogen | Hydrogen | Hydrogen | Hydrogen | Argon | Argon | Argon |

DEW POINT, °C

| -55 | -55 | -55 | -55 | -67 | -67 | -72 |

Fig. 2.5 — 0.010-inch-thick Mo-A specimens stress-rupture tested at 2200°C
(Neg. P62-11-4)

The data summary in Table 2.2 indicates an increase in the stress-rupture life of tantalum as the dewpoint of the argon is increased. This is attributed to a more active tungsten-water vapor reaction at the higher moisture levels which results in larger amounts of tungsten or tungsten oxide being transported to the specimen, thereby yielding increased strength. This effect on stress-rupture properties is quite similar although not as pronounced as that observed with molybdenum tested in argon. Chemical analyses are now in progress to evaluate these anticipated differences in contamination. If this mechanism is confirmed, the scatter obtained in the argon tests can be attributed to dewpoint variations between tests.

The tantalum results obtained in the two different hydrogen atmospheres were essentially identical. Obviously, differences in the impurity levels of the hydrogen exhibit a very minimal effect on this material under these conditions.

The above considerations emphasize the importance of employing noble gases of extremely low (-75°C) dewpoints for use in high-temperature testing of refractory metals.

No. 1	No. 2	No. 3	No. 4	No. 5	No. 6

INITIAL STRESS, psi

600	500	400	600	500	400

TIME TO RUPTURE, hours

1.5	3.2	6.7	1.3	3.0	5.6

PERCENT ELONGATION IN 1-INCH GAUGE LENGTH

49.5	47.5	50.4	54.2	59.4	37.2

TEST ATMOSPHERE

Hydrogen	Hydrogen	Hydrogen	Argon	Argon	Argon

DEW POINT, °C

	−55	−56		−67	−64
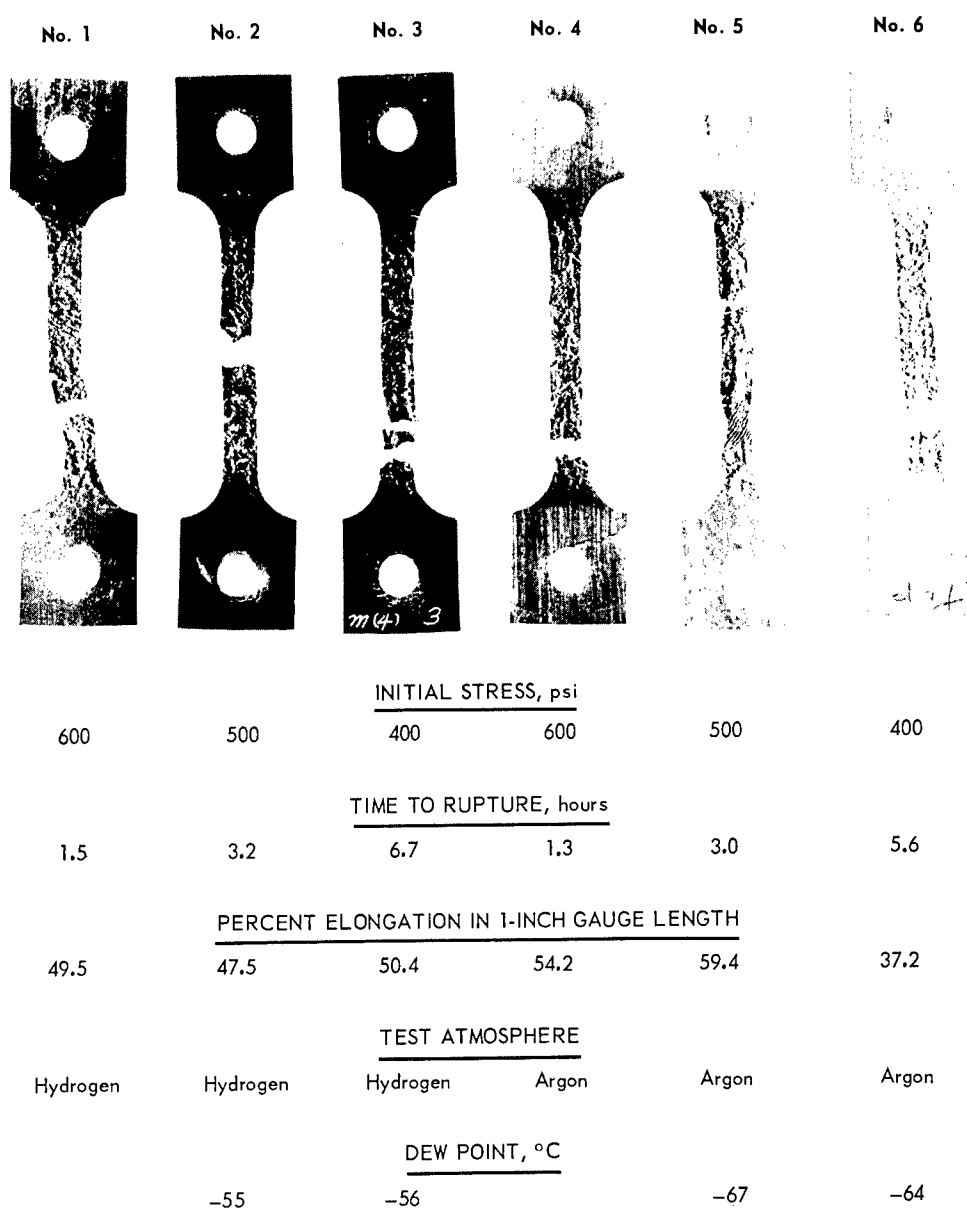
Fig. 2.6 — 0.011-inch-thick Mo-B specimens stress-rupture tested at 2200°C (Neg. P62-11-8A)
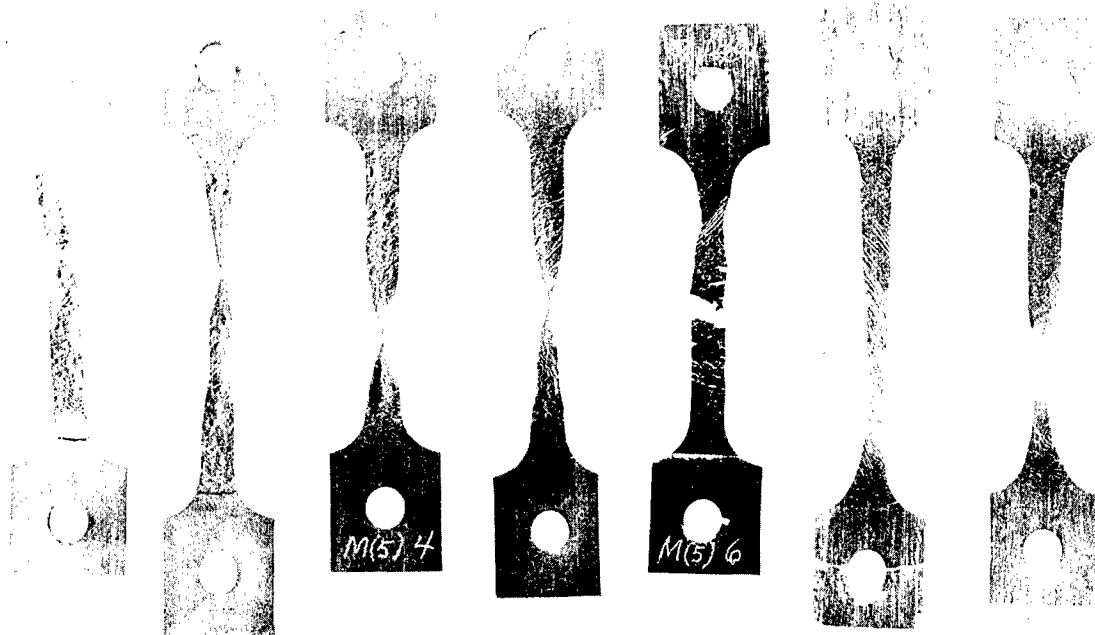
No. 2	No. 3	No. 4	No. 5	No. 6	No. 7	No. 8

			INITIAL STRESS, psi			
750	600	450	550	450	550	700

			TIME TO RUPTURE, hours			
0.5	1.3	2.7	1.5	3.2	1.9	0.4

		PERCENT ELONGATION IN 1-INCH GAUGE LENGTH				
57.2	105.5	64.0	90.5	47.2	103.8	78.0

			TEST ATMOSPHERE			
Hydrogen	Hydrogen	Hydrogen	Hydrogen	Argon	Argon	Argon

			DEW POINT, °C			
--	--	−52	−54	−72	−72	--

Fig. 2.7 — 0.015-inch-thick Mo-C specimens stress-rupture tested at 2200°C
(Neg. P62-11-8B)

TABLE 2.2

EFFECT OF ATMOSPHERE ON TANTALUM STRESS-
RUPTURE TESTS AT 2600°C AND 170 PSI

Atmosphere	Dewpoint, °C	Rupture Time, hr	Percent Elongation In 1-Inch Gage Length
Argon[a]	-59	5.03	45
Argon[a]	-65	3.83	58
Argon[b]	-79	2.33	47
Argon[b]	-79	2.81	40
Hydrogen[a]	-54	2.05	40
Hydrogen[a]	-53	2.06	36
Hydrogen[c]	-79	2.67	57
Hydrogen[c]	-79	2.23	30

[a]Plant distribution system.
[b]Bottled liquid argon.
[c]Bottled high purity hydrogen.

Hydrogen is shown to be an attractive test atmosphere for such measurements, particular-
ly since the tungsten-water vapor cycle is almost completely suppressed by the hydrogen.

Analysis of Creep Measurements

Further analysis of the total elongation measurements obtained during the stress-rupture
tests is being made in order to obtain a preliminary evaluation of creep behavior. As previ-
ously reported[*] a plot of log initial stress versus log linear creep rate for Ta - 10W at 2600°C
and 2800°C was linear with a slope of approximately 0.25 yielding an exponent on stress in
the Weertman[†] equation equal to about 4.0. This was pointed out as being very close to the
stress relationship developed by Weertman for dislocation climb. Data for several addi-
tional materials are presented in Figure 2.8 and are seen to follow the same relationship,
i.e., a slope of 0.25. An exception is noted in the case of Mo-A which has a slope close
to 0.6. While the exact cause of this different creep-dependence on stress is unidentified,
this difference is reflected in the stress-rupture data. Creep analyses[‡] have shown that
the slope of the lines in Figure 2.8 should be equal to that of the corresponding line in Fig-
ure 2.1 except of opposite sign. Therefore the different slopes obtained in Figure 2.1 for
different molybdenum materials should be reflected as different slopes in the creep rate
plot of Figure 2.8. These data provide a measure of the reproducibility and accuracy of
the testing in this program.

WORK PLANNED FOR NEXT PERIOD

Stress-rupture testing at 2200°, 2400°, 2600°, and 2800°C will be continued on refrac-
tory alloys in hydrogen and argon, and initiated in neon.

Creep measurements within the specimen gage section will be made on a selective basis
to confirm the creep analyses mentioned above based on elongation measurements.

Longer time (100 hour) stress-rupture tests will be performed to determine the validity
of extrapolating current 10-hour data.

---

[*]"High-Temperature Materials Program Progress Report No. 17, Part A," GE-NMPO, GEMP-17A, November 15, 1962,
pp. 26–28.
[†]J. Weertman, Journal of Applied Physics, Volume 26, 1955, p. 1213.
[‡]J. B. Conway, "Presentation, Correlation, and Interpretation of High-Temperature Stress Rupture and Creep Data,"
GE-NMPO, TM 62-11-14, November 1962.
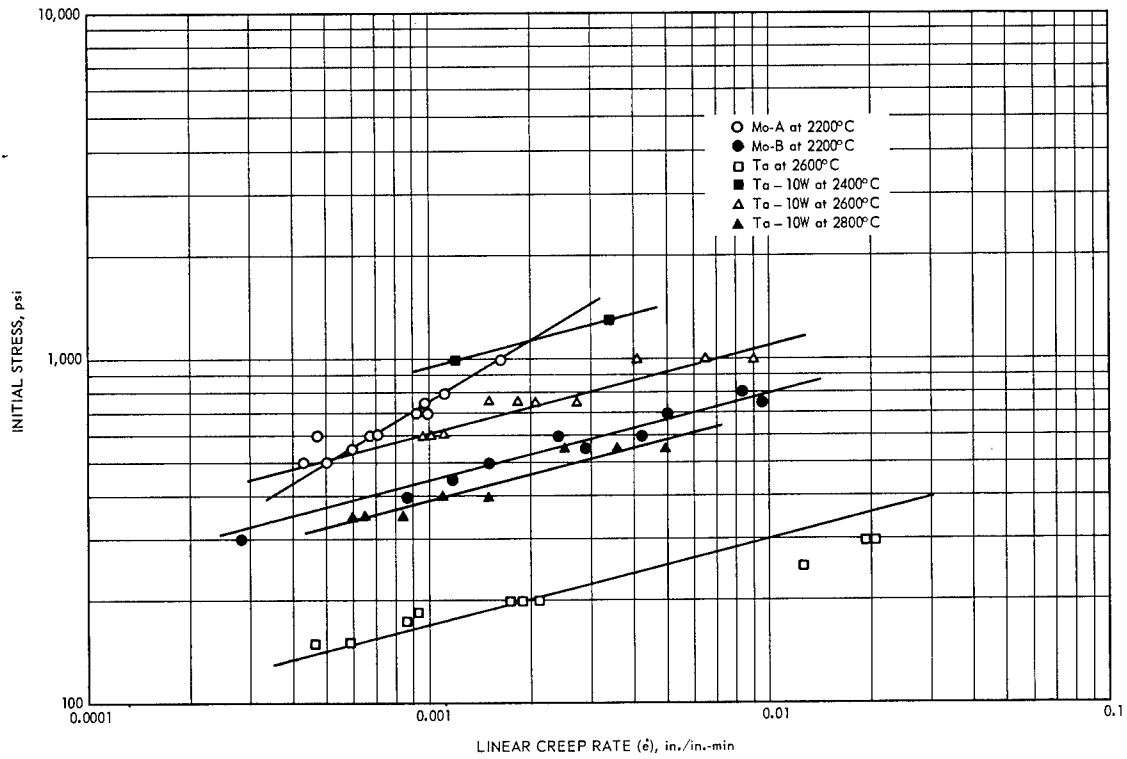
Fig. 2.8 — Initial stress versus linear creep rate in hydrogen

3. EFFECT OF RADIATION ON HIGH-TEMPERATURE ALLOYS

(57004)

The objective of this program is to determine the effect of radiation on the time-, temperature-, and stress-dependent properties of selected high-temperature alloys and refractory metals, to identify the causes of any observed changes in these properties, and to develop remedial measures.

REFRACTORY METALS EXPERIMENTAL PROGRAM

A program to study the influence of neutron irradiation on refractory metals and their alloys has been initiated. This program will follow the eleven high-temperature alloy experiments based on A-286, Hastelloy X, and Rene' 41 materials. The refractory metals program will be the major experimental effort for Calendar Year 1963 with only a few concluding experiments to be performed on the high-temperature alloys.

The objective of the refractory metals program is to determine the relative effects of irradiation on the physical and mechanical properties of these materials. Primary emphasis will be placed on establishing damage mechanisms and remedial measures. The major effort will be conducted on tungsten and tungsten-base alloys with a limited effort, primarily for background information, on molybdenum, molybdenum-base alloys, and other body-centered metals.

The physical and mechanical tests will include creep-rupture, tensile, brittle-ductile transition temperature, hardness, and resistivity. Other tests may be included, as deemed necessary, to help establish damage mechanisms. Emphasis will be placed on the influence of grain size in radiation effects. An investigation of the effect of various post-irradiation heat treatments on the properties of refractory metals is planned. Both isochronel and isothermal annealing studies will be performed. The use of materials of several purity levels, including one of extremely high purity, is also being considered. Initial creep-rupture tests will be conducted at approximately $1650^{\circ}C$. Tensile testing will be performed at room and at elevated temperatures.

An initial exploratory study of the creep-rupture properties of refractory metals is in progress. Molybdenum and tungsten specimens were irradiated at reactor ambient temperatures to a neutron dosage of approximately 3×10^{17} and 3×10^{18} nvt ($E_n \geq 1$ Mev), respectively. The predicted induced activities of some refractory metals are shown in Figure 3.1. The experimental data for tungsten and molybdenum will be compared at a later time. For the present, the experimental program on tantalum and tantalum-base alloys will be kept to a minimum due to the long residual induced radioactivity.

Two creep-rupture stands used in the FY-62 program are being modified for the refractory metal program. A furnace designed for tensile or stress-rupture testing up to $1780^{\circ}C$ will be installed. The furnace will be equipped to test specimens in hydrogen,
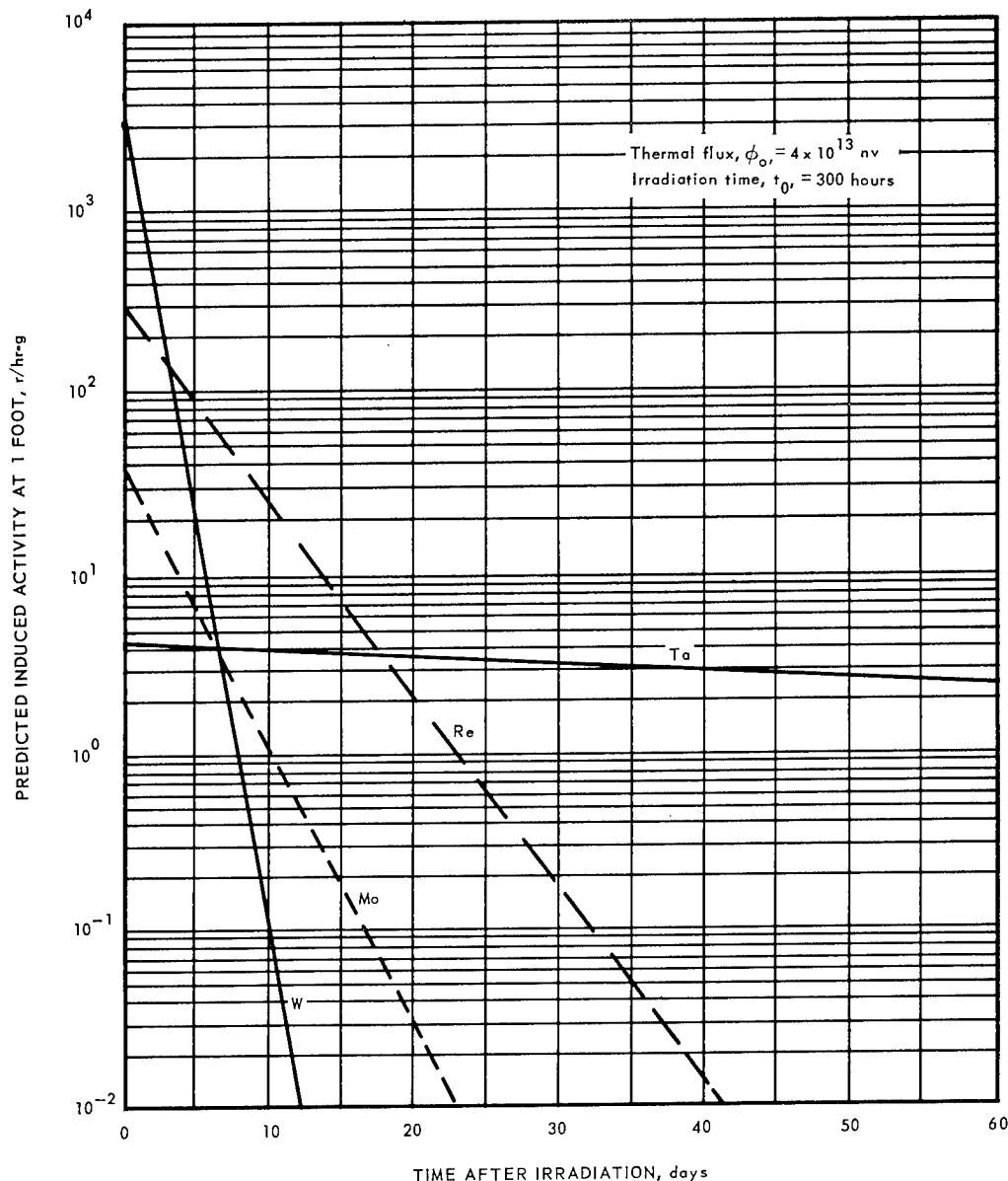
Fig. 3.1 — Induced activity of refractory metals as a function of decay time

inert gas, or in vacuum. It will employ a circular molybdenum heating element. Tungsten heating elements will be prepared for later installation. It is planned to have this furnace in operation early in the next report period.

Specimen Preparation

Commercially pure 0.135- and 0.200-inch diameter tungsten rods were received for the preliminary investigation. Metallographic examinations and density measurements were completed; complete chemical analyses are in progress. Three 40-inch lengths of 0.135-inch-diameter W - 25Re rod were also received and are being evaluated. The preliminary designs of the specimens for the refractory metals program are shown in Figure 3.2. The flat specimens will be used in the initial work since extensive control data exists for the refractory metals based on this specimen type. Based on the comparison of the round and the flat irradiated specimens data, one design will be selected for the major

THICKNESS RANGE – 0.010 TO 0.020

FLAT SPECIMEN

ALL DIMENSIONS IN INCHES

ROUND SPECIMENS
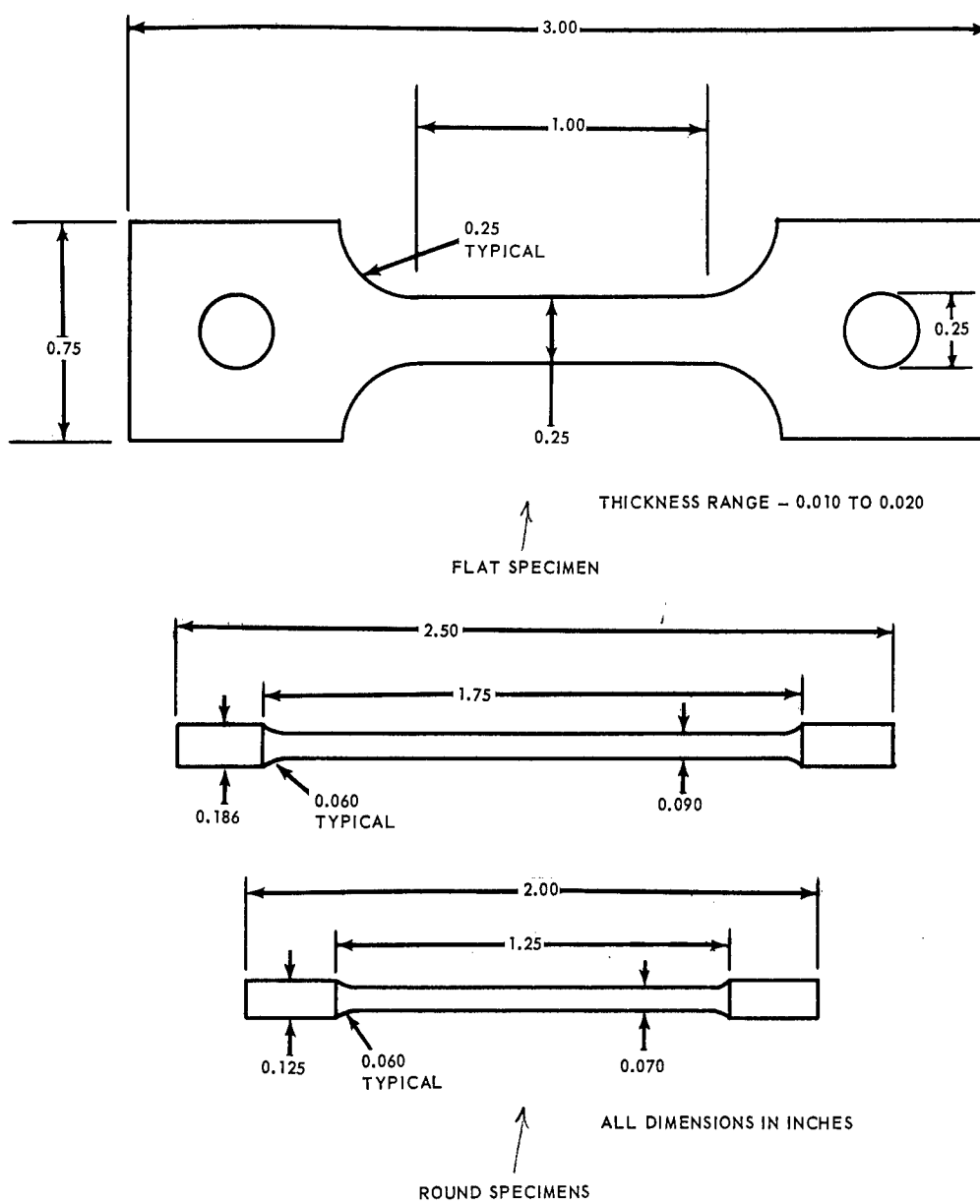
Fig. 3.2 – Preliminary design of refractory metal specimens for creep, stress-rupture, and tensile testing

testing program on refractory metals. Manufacture of specimens and load train hard-
ware from tungsten is in progress and will be completed within the next reporting period.

The surface condition of tungsten specimens is known to affect its mechanical properties.*†
A limited exploratory study was conducted to investigate the techniques required for electro-
polishing tungsten. Equipment, as shown in Figure 3.3, was assembled and installed. This
apparatus permits both rotating the specimen and stirring the electrolyte. Polishing condi-
tions, similar to those of another investigation,‡ include the following:

1. Electrolyte, 2 percent sodium hydroxide
2. Current density, 3 to 6 amp/sq. in.
3. Rotation of specimen, 3 rpm
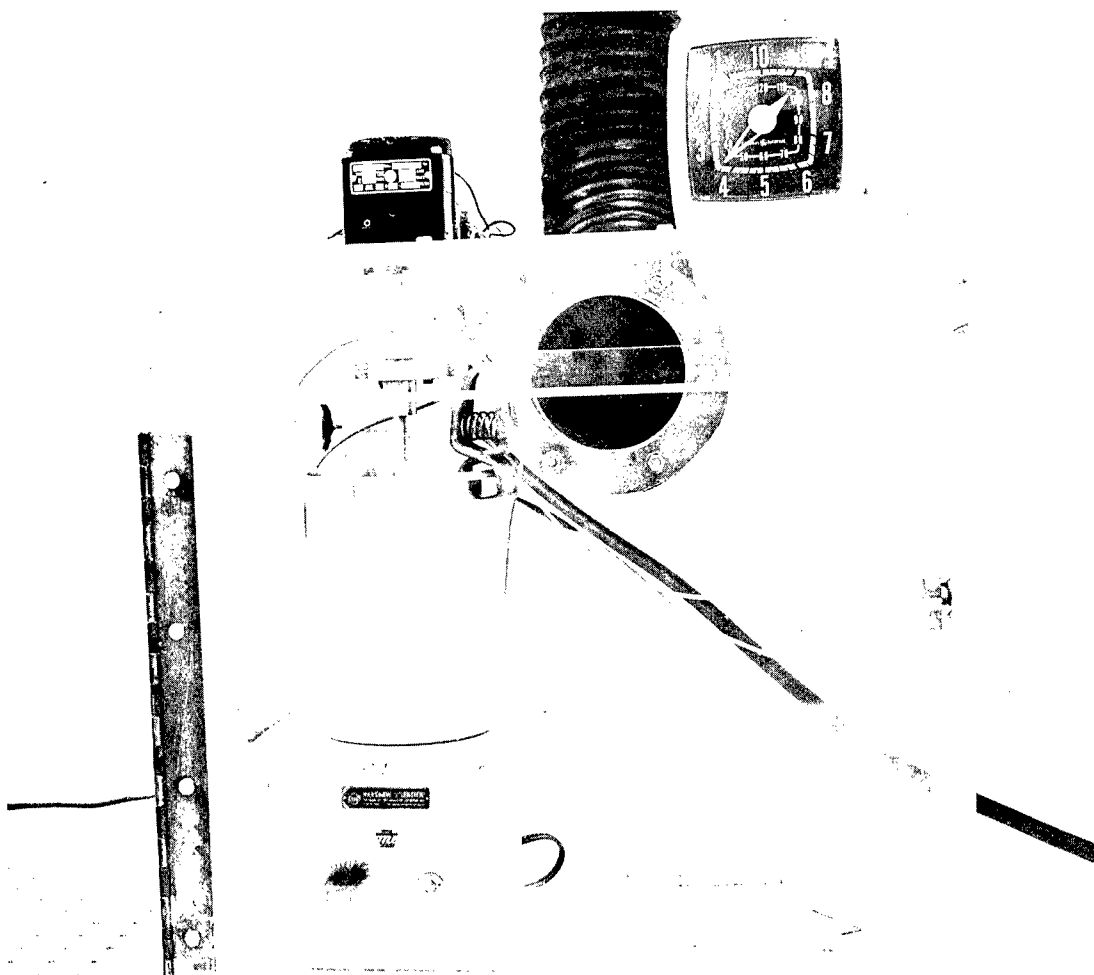
Fig. 3.3 — Refractory metal specimen surface electropolishing apparatus
(Neg. P62-12-5B)

*K. Sedlatschek, and D. A. Thomas, "The Effect of Surface Treatment on the Mechanical Properties of Tungsten,"
Powder Metallurgy Bulletin, Vol. 8, Nos. 1—2, June 1957, pp. 35—40.
†J. R. Stephan, "Effect of Surface Condition on Ductile-To-Brittle Transition Temperature of Tungsten," NASA
TN D-676, Lewis Research Center, February 1961.
‡J. R. Stephan, "An Exploratory Investigation of Some Factors Influencing The Room-Temperature Ductility of
Tungsten," NASA TN D-304, Lewis Research Center, August 1960.

4. Cathode, stainless steel beaker (1. 5 qt. , 4 inch I. D.) centered about the rotating specimen
5. Temperature of electrolyte, 25°C

The bottom of the beaker is fitted with a Teflon disc to prevent reaction and gas evolution.

Limited experimentation with tungsten specimens have demonstrated that it is possible to electropolish the surface from approximately a 24 microinch RMS ground finish to a highly polished surface of 2 to 5 microinch RMS finish. Rates of metal removal are relatively rapid, approximately 0. 5 to 1. 0 mil from the gage diameter per minute. Figure 3. 4 shows the finish of machined tungsten before and after electropolishing.

HIGH-TEMPERATURE ALLOYS EXPERIMENTAL PROGRAM

Status of Irradiation Program

The status of the experimental program is summarized in Table 3. 1.

Test capsule MT-99, containing smooth stress-rupture specimens of A-286 alloy, was prepared and shipped to GE-ITS for irradiation. These specimens will be used (Experiment No. 6) for the determination of the effect of neutron reactions with the trace quantities of boron present in this alloy. There are four groups of seven specimens each. The first three groups, from the same heat, contain 0. 00085, 0. 00425, and 0. 010 weight percent natural boron. The fourth group of seven specimens contains 0. 0065 weight percent boron which is depleted in the boron-10 isotope. The test capsule will be inserted in the K-3 hole of the ETR and will be irradiated at reactor ambient temperatures for two cycles. The capsule is instrumented with nickel-cobalt flux monitors attached to center rods.

Capsule LTTS-18 irradiations were completed in the Graphite Pile facility at Oak Ridge. This capsule contains the A-286 test specimens that will be used in the relaxation tests (Experiment No. 9). The capsule will be removed from the reactor the first week of the next reporting period and the specimens shipped to Evendale. Testing of control specimens will be initiated following evaluation of the irradiation temperature data. The capsule was irradiated approximately 490 hours at a temperature greater than 620°C. The temperature gradient along the specimen length in stage 1 was approximately 80°C and 30°C in stage 2. The nominal temperature difference between the two stages was approximately 45°C.

The irradiation plans for Rene' 41 relaxation specimens have not been established pending evaluation of the A-286 specimens. In order to place greater effort on the new refractory metals program, the Rene' 41 portion of experiment 9 is being postponed indefinitely.

Post-Irradiation Testing

Stress-Rupture Results for Experiment No. 4 - Experiment No. 4 was conducted to evaluate the effects of irradiation on the precipitation hardening alloys A-286 and Rene' 41 in the underaged and the overaged heat treated condition. The post-irradiation test results for the A-286 alloy were reported previously.*

The Rene' 41 test data are presented in Table 3. 2 and Figure 3. 5. These specimens were irradiated in Capsule MT-38 at approximately 650°C. The overaged control data indicates higher rupture strengths than those of the underaged specimens. A similar effect was noted for the irradiated specimens. Both the control and the irradiated overaged and underaged test data indicate lower rupture strengths than the data obtained from test specimens† given the standard heat treatment. It is interesting to note that the underaged control

---

*"High-Temperature Materials Program Progress Report No. 9, Part A," GE-NMPO, GEMP-9A, March 30, 1962, p. 44.
†"High-Temperature Materials Program Progress Report No. 11, Part A," GE-NMPO, GEMP-11A, May 15, 1962, p. 53.

Fig. 3.4 — Polished and unpolished tungsten specimen (Neg. P62-12-4)

TABLE 3.1

SUMMARY OF EXPERIMENTAL PROGRAM

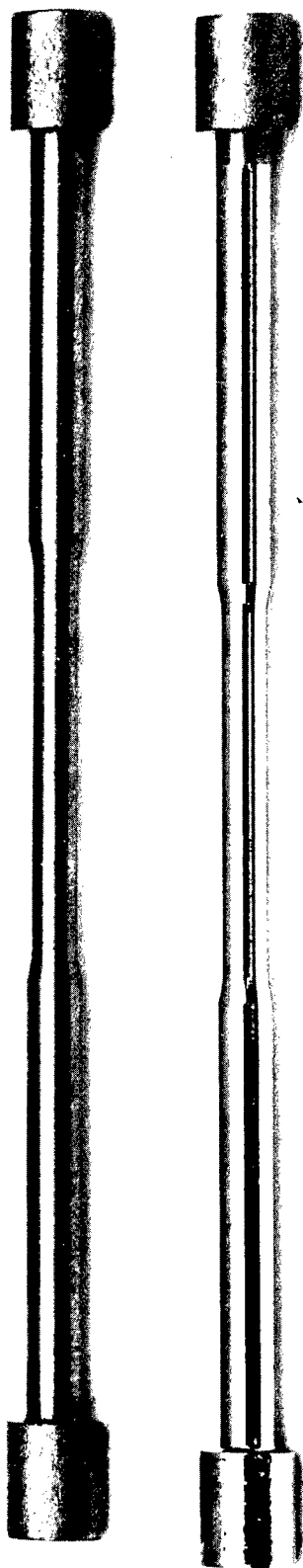| Experiment No.	Objective	Alloys	Capsule	Irradiation Conditions — Approximate Temperature, °C	Approximate Dosage, nvt ($E_n \geq 1$ Mev)	Heat	Temperature, °C	Rupture Strength, 1000 psi — 100 Hours — Control	Irradiated	1000 Hours[a] — Control	Irradiated
1	To investigate the effects of neutron irradiation on the tensile and stress rupture properties of high-temperature alloys receiving the standard heat treatment for these experiments. To generate the background data needed on these alloys for comparison with other experiments	A-286	MT-27	540	7×10^{19}	C2527	540	100	93	82	77
			MT-38	650	5×10^{19}	C2527	650	54	38	41	22
			MT-43	650	11×10^{19}	B15649	650	52	37	35	19
			MT-43	650	11×10^{19}	7611 & 12878	650	49	34	31	18
		Hastelloy X	MT-27	540	7×10^{19}	E9500	540	66	55	54	44
			MT-38	650	5×10^{19}	E9500	650	43	37	27	27
			MT-43	650	11×10^{19}	X1-4385	650	43	42	30	32
			MT-51	870	4×10^{19}	E9500	870	9	8	4	5.5
			MT-51	870	4×10^{19}	E9500	650	41	-	27	-
		Rene' 41	MT-38	650	5×10^{19}	TV746	650	107	85	87	67
			MT-43	650	11×10^{19}	TV754	650	124	101	101	77
			MT-51	870	4×10^{19}	TV754	870	23	18	12	13
			MT-51	870	4×10^{19}	TV754	650	-	104	-	92
2	To investigate the effect on the stress rupture properties of a standard heat treatment following neutron irradiation.	A-286	MT-27	540	7×10^{19}	C2527	540	97	86	76	65
			MT-38	650	5×10^{19}	C2527	650	54	31	40	17
		Hastelloy X	MT-27	540	7×10^{19}	E9500	540	61	66[b]	52	57[b]
			MT-38	650	5×10^{19}	E9500	650	39	35	25	23
			MT-51	870	7×10^{19}	E9500	870	9.5	6.5	5.5	3
		Rene' 41	MT-38	650	5×10^{19}	TV746	650	105	92	93	87
			MT-51	870	4×10^{19}	TV754	870	26	11	12	4
3	To investigate the role of grain size and other related structural characteristics in the possible mechanisms of neutron-induced stress rupture property changes.	A-286	MT-43	650	11×10^{19}	B15649	650	57	42	43	28
		Rene' 41	MT-43	650	11×10^{19}	TV754	650	120	91	96	66
			MT-51	870	4×10^{19}	TV754	870	20[b]	11[b]	13[b]	8[b]
4	To investigate the effect of the degree of pre-irradiation aging on the stress rupture properties of irradiated alloys.	A-286	MT-27	540	7×10^{19}	7611	540	96	80	74	70
			MT-38	650	5×10^{19}	7611	650	52	41	40	28
		Rene' 41	MT-38	650	5×10^{19}	TV746	650	Testing completed. See Figures 3.5 and 3.6.			
			MT-51	870	4×10^{19}	TV746	870	-	-	-	-
5	To determine whether some parameter that is a function of thermal neutrons has an effect on stress rupture properties.	A-286	MT-35	36	3.0×10^{16}	C2527	650	57	54	38	35
					12.0×10^{16}[c]	C2527	650	57	54	38	35
			MT-36	36	3.0×10^{16}	C2527	650	57	46	38	30
					12.0×10^{16}[c]	C2527	650	57	46	38	30
6	To investigate the effect of neutron reactions with trace quantities of boron generally present in alloys on their stress rupture properties.	A-286	MT-99	Ambient	7×10^{20}	-	650	Shipped to ITS. Scheduled for irradiation about January 7, 1963.			
7	To determine whether neutron irradiation at reactor ambient temperature induces strain rate embrittlement.	A-286	LTTS-15	36	3×10^{19}	C2527	25	Irradiation completed. Testing in progress. Control specimens testing approx. 90% complete.			
		Hastelloy X	LTTS-15	36	3×10^{19}	E9500	25				
		Rene' 41	LTTS-15	36	3×10^{19}	TV746	25				
8	To determine the fast neutron threshold of radiation-induced changes for stress rupture properties of high temperature alloys.	A-286	LTTS-17	650	8.3×10^{14}	B15649	650	52	50[d]	35	32[d]
			LTTS-16	650	2.7×10^{16}	B15649	650	52	42[d]	35	25[d]
		Hastelloy X	LTTS-17	650	8.3×10^{14}	E9500	650	43	42	27	27
			LTTS-16	650	2.7×10^{16}	E9500	650	43	37	27	27
		Rene' 41	LTTS-17	650	8.3×10^{14}	TV754	650	124	124[d]	101	101[d]
			LTTS-16	650	2.7×10^{16}	TV754	650	124	113[d]	101	90[d]
9	To investigate the effect of neutron irradiation on the relaxation properties of high-temperature alloys.	A-286	LTTS-18	650	10^{19}	B15649	-	Irradiation complete. To be shipped to Evendale.			
10	To investigate the effect of neutron irradiation on the high-temperature fatigue properties of high-temperature alloys.	A-286	MT-51	540	4×10^{19}	B15649	540	-	-	-	-
			MT-51	650	4×10^{19}	B15649	650	69[e]	-	56[f]	-
		Rene' 41	MT-51	650	4×10^{19}	TV746	650	-	-	-	-
11	To investigate the effect of neutron irradiation on the stress rupture properties of welded joints of high-temperature alloys.	Hastelloy X	MT-51	870	4×10^{19}	E9500	870	8	7.5	3.5	-
			LTTS-14	650	4×10^{19}	E9500	650	44	35	32	25
		Rene' 41	MT-51	870	4×10^{19}	TV850	870	25.5	14	15	5.6

[a]Extrapolation data.
[b]Tentative data based on partially completed experiment.
[c]Thermal flux.
[d]Approximate.
[e]Stress value listed is the endurance limit for 10^7 cycles.
[f]Stress value listed is endurance limit for 10^8 cycles.

TABLE 3.2

STRESS RUPTURE PROPERTIES OF RENE' 41 AT 650°C
EXPERIMENT NO. 4

Specimen[a]	Stress, psi	Rupture Time, hr	Elongation, % in 1.5 in.	Reduction Of Area, %
Controls - Simulated cycle, 100 hours at 650°C:				
Overaged[b]				
29R	100,000	140.5	2.8	4.9
30R	95,000	178.4	6.9	7.8
Underaged[c]				
19R	100,000	30.6	1.3	0.8
20R	95,000	29.0	1.1	0.8
Irradiated at 650°C in MT-38:				
Overaged[b]				
26R	90,000	45.6	1.6	3.2
28R	82,000	110.0	2.0	6.3
Underaged[c]				
16R	90,000	3.0	1.7	6.3
17R	85,000	1.5	0.9	3.2
18R	70,000	7.4	1.6	nil

[a]All specimens were of the smooth-bar type from Heat TV-746.
[b]Heat treatment prior to grinding:
  1205°C - 2 hr - water quench
  1065°C - 6 hr - water quench
   925°C - 48 hr - air cool
   760°C - 100 hr - air cool
[c]Heat treatment prior to grinding was the same as the underaged
  specimens plus 1175°C for 1/2 hr and cooled to 25°C in argon.
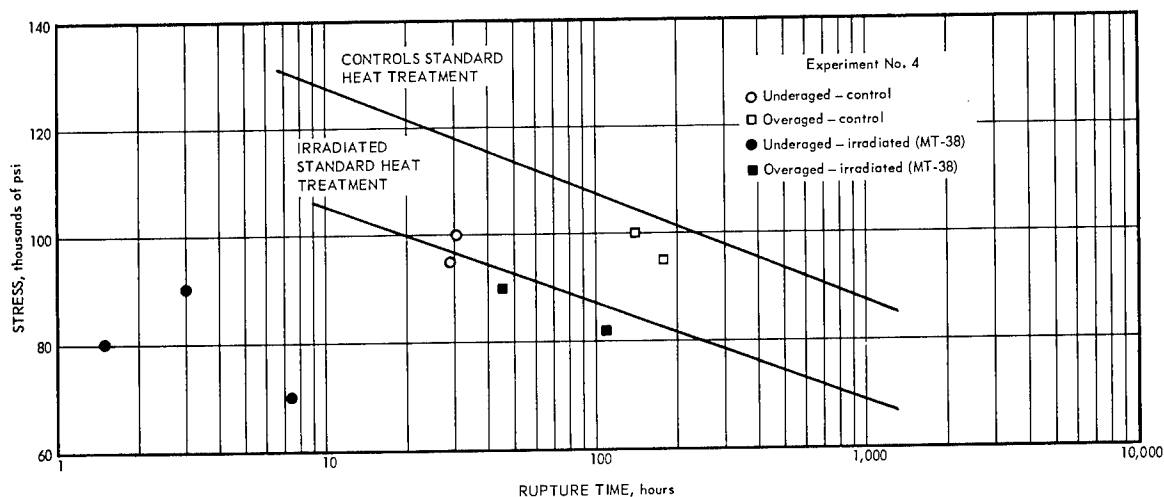
Fig. 3.5 — Stress-rupture properties of Rene' 41 at 650°C — Heat TV-746,
Capsule MT-38

specimen data appear to have rupture strengths comparable to the irradiated specimens which received the standard heat treatment prior to irradiation.

The Rene' 41 data for specimens irradiated at 870°C in Capsule MT-51 and post-irradiation tested at the same temperature are listed in Table 3.3 and plotted in Figure 3.6. The control test data indicated no significant differences, based on the few specimens tested, between the overaged and the underaged heat treatment, and, therefore, the data were grouped in the curve fitting. As reported in the 650°C tests, the irradiated overaged specimen test data show greater rupture strengths than the underaged specimen data. The data seem to indicate that there is some annealing of radiation effects with time at temperature at the lower stresses.

Tensile Test Results for Experiments No. 1, 2, and 3 - Rene' 41 test specimens from two heats (TV-746 and TV-754) were used in Experiments No. 1, 2, and 3. The specimens in Heat TV-746 were fabricated from 3/8-inch plate stock,* while those of Heat TV-754 were fabricated from 7/16-inch round stock.* The tensile data for the control and irradiated test specimens are listed in Tables 3.4 to 3.7. The marked variations in the tensile properties between specimens of the two heats make it desirable to examine the results separately.

TABLE 3.3

STRESS RUPTURE PROPERTIES OF RENE' 41 AT 870°C
EXPERIMENT NO. 4

Specimen[a]	Stress, psi	Rupture Time, hr	Elongation, % in 1.5 in.	Reduction Of Area, %
Controls - Simulated cycle, 100 hours at 870°C				
Overaged[b]				
34R	35,000	9.3	10.5	30.2
35R	16,000	1200.5[d]	12.0	25.9
Underaged[c]				
24R	35,000	28.5	7.5	19.8
25R	20,000	444.6	15.3	38.3
Irradiated at 870°C in MT-51:				
Overaged[b]				
31R	25,000	7.0	0.7	4.7
32R	10,000	4191.0[e]	2.2	-
33R	17,500	223.4	1.9	6.3
Underaged[c]				
21R	25,000	4.0	1.1	1.5
22R	15,000	32.4	1.2	9.4
23R	10,000	1035.3[f]	2.3	-

[a]All specimens were of the smooth-bar type from Heat TV-746.
[b]Heat treatment prior to grinding:
   1205°C - 2 hr - water quench
   1065°C - 6 hr - water quench
   925°C - 48 hr - air cool
   760°C - 100 hr - air cool
[c]Heat treatment prior to grinding was the same as above plus 1175°C
   for 1/2 hr and cooled to 25°C in argon.
[d]Equivalent time at 870°C based on 43.3 hr at 890°C and 1045.5 hr
   at 870°C.
[e]Equivalent time at 870°C based on 1003 hr at 890°C and 575 hr at
   870°C.
[f]Equivalent time at 870°C based on 98.6 hr at 890°C and 698 hr at
   870°C.

*"High-Temperature Materials Program Progress Report No. 13, Part A," GE-NMPO, GEMP-13A, July 31, 1962,
   Table 5.2, p. 34.

TABLE 3.4

RENE' 41 CONTROL SPECIMEN TENSILE TEST DATA
EXPERIMENTS 1, 2, AND 3

Specimen[a]	Test Temperature, °C	0.2-Percent Yield, psi	Ultimate Strength, psi	Elongation, %	Reduction Of Area, %	Pre-Treatment Temperature, °C	Pre-Treatment Time, hr	Pre-Treatment Quench/Cool	Pre-Test Treatment Temperature, °C	Pre-Test Treatment Time, hr	Pre-Test Treatment Cool/Quench
Smooth Specimens											
110RS[b]	650	126,700	188,600	10.7	8.0	1065 / 1065 / 760	2 / 1/2 / 16	Water / Air / Air	650	100	Air
111RS[b]	650	134,500	195,000	13.5	13.8	1065 / 1065 / 760	2 / 1/2 / 16	Water / Air / Air	650	100	Air
112RS[b]	870	35,300	61,400	20.7	48.8	1065 / 1065 / 760	2 / 1/2 / 16	Water / Air / Air	870	100	Air
154RS[b]	870	46,000	68,400	24.7	62.5	1065 / 1065 / 760	2 / 1/2 / 16	Water / Air / Air	870	100	Air
93RS	26	150,700	199,000	9.9	8.3	1065 / 1175 / 900	2 / 1/2 / 4	Water / Air / Air	650	100	Air
97RS	650	133,700	192,800	11.6	9.8	1065 / 1175 / 900	2 / 1/2 / 4	Water / Air / Air	650	100	Air
98RS	650	130,400	187,600	14.4	13.8	1065 / 1175 / 900	2 / 1/2 / 4	Water / Air / Air	650	100	Air
140RS	870	45,600	68,300	22.9	53.7	1065 / 1175 / 900	2 / 1/2 / 4	Water / Air / Air	870	100	Air
149RS	26	135,100	161,300	2.0	3.0	1065 / 1175 / 900	2 / 1/2 / 4	Water / Air / Air	870	100	Air
150RS	650	114,200	180,200	4.1	5.4	1065 / 1175 / 900	2 / 1/2 / 4	Water / Air / Air	870	100	Air
151RS	870	54,200	79,500	26.7	60.4	1065 / 1175 / 900	2 / 1/2 / 4	Water / Air / Air	870	100	Air

TABLE 3.4 (Contd.)

RENE' 41 CONTROL SPECIMEN TENSILE TEST DATA
EXPERIMENTS 1, 2, AND 3

Specimen[a]	Test Temperature, °C	0.2-Percent Yield, psi	Ultimate Strength, psi	Elongation, %	Reduction Of Area, %	Pre-Treatment Temperature, °C	Time, hr	Quench/Cool	Pre-Test Treatment Temperature, °C	Time, hr	Cool/Quench
99RS	870	-	76,200	4.8	33.0	1065	2	Water	870	100	Air
						1175	1/2	Air	1065	2	Water
						900	4	Air	1175	1/2	Air
									900	4	Air
100RS	870	64,200	75,400	11.4	24.0	1065	2	Water	870	100	Air
						1175	1/2	Air	1065	2	Water
						900	4	Air	1175	1/2	Air
									900	4	Air
148RS	870	75,700	83,800	20.5	39.3	1065	2	Water	870	100	Air
						1175	1/2	Air	1065	2	Water
						900	4	Air	1175	1/2	Air
									900	4	Air
Notched Specimens											
35RN[b]	650	-	233,400	-	-	1065	2	Water	650	100	Air
						1065	1/2	Air			
						760	16	Air			
36RN[b]	650	-	234,400	-	-	1065	2	Water	650	100	Air
						1065	1/2	Air			
						760	16	Air			
31RN	26	-	235,600	-	-	1065	2	Water	650	100	Air
						1175	1/2	Air			
						900	4	Air			
32RN	26	-	233,500	-	-	1065	2	Water	650	100	Air
						1175	1/2	Air			
						900	4	Air			
33RN	650	-	220,200	-	-	1065	2	Water	650	100	Air
						1175	1/2	Air			
						900	4	Air			
39RN	870	-	119,000	-	-	1065	2	Water	870	100	Air
						1175	1/2	Air			
						900	4	Air			

[a]All specimens are from Heat TV-754.
[b]Experiment No. 3.
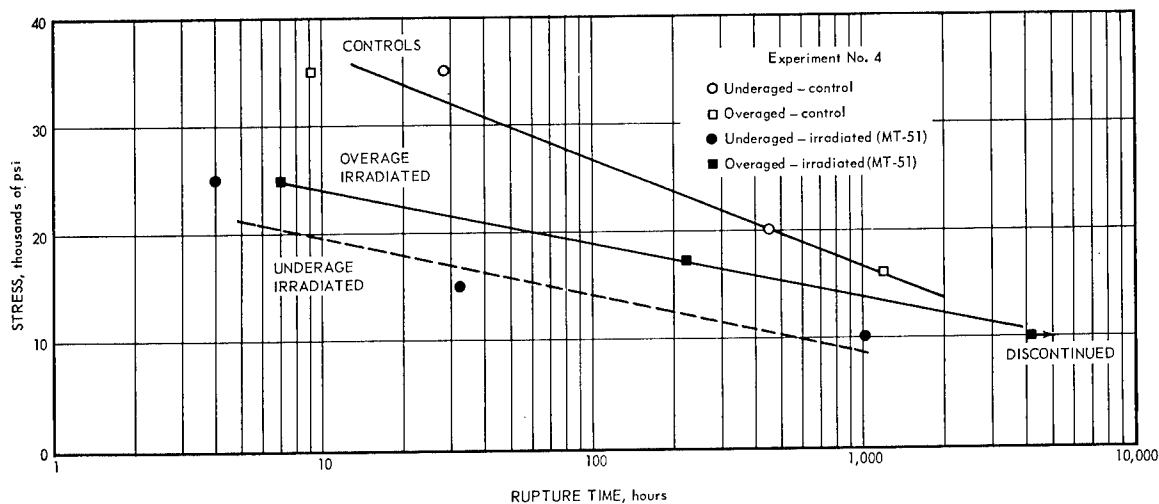
Fig. 3.6 — Stress-rupture properties of Rene' 41 at 870°C — Heat TV-746, Capsule MT-51

TABLE 3.5

RENE' 41 CONTROL SPECIMEN TENSILE TEST DATA
EXPERIMENTS 1 AND 2

Specimen[a]	Test Temperature, °C	0.2-Percent Yield, psi	Ultimate Strength, psi	Elongation, %	Reduction Of Area, %	Pre-Test Treatment		
						Temperature, °C	Time, hr	Cool/Quench
Smooth Specimens								
11RS	26	99,700	147,000	12.5	12.4	540	100	Air
33RS	26	105,000	144,000	10.6	12.3	540	100	Air
34RS	540	94,500	127,000	10.0	14.0	540	100	Air
35RS	540	95,000	133,000	12.0	17.7	540	100	Air
51RS	26	117,000	137,000	3.3	4.8	650	100	Air
52RS	540	110,000	134,000	5.6	12.5	650	100	Air
53RS	650	103,000	145,000	10.3	13.9	650	100	Air
141RS	650	101,900	142,900	14.2	11.4	650	100	Air
41RS	540	89,600	133,000	14.8	13.9	650	100	Air
						1065	2	Water
						1175	1/2	Air
						900	4	Air
54RS	650	89,600	137,000	14.6	15.4	650	100	Air
						1065	2	Water
						1175	1/2	Air
						900	4	Air
36RS	650	84,800	136,000	15.0	18.3	650	100	Air
						1065	2	Water
						1175	1/2	Air
						900	4	Air
Notched Specimens								
26RN	26	-	168,000	-	-	540	100	Air
27RN	540	-	180,000	-	-	540	100	Air
11RN	26	-	171,000	-	-	As-machined		
28RN	540	-	202,000	-	-	650	100	Air
29RN	650	-	187,000	-	-	650	100	Air

[a]All specimens from Heat TV-746, which were heat treated prior to grinding: 1065°C for 2 hr
and water quenched plus 1175°C for 2 hr and air cooled plus 900°C for 4 hr and air cooled.

TABLE 3.6

RENE' 41 IRRADIATED SPECIMEN TENSILE TEST DATA, EXPERIMENTS 1, 2, AND 3

Specimen[a]	Pre-Irradiation Treatment			Capsule	Irradiation Conditions			Test Temperature, °C	0.2-Percent Yield, psi	Ultimate Strength, psi	Elongation, %	Reduction Of Area, %
	Temperature, °C	Time, hr	Quench/Cool		Dosage, nvt (En ≥ 1 Mev)	Temperature, °C	Time, hr					
Smooth Specimens												
28RS[c]	1065	2	Water	MT43	0.6×10^{20}	675	67.2	650	145,060	183,350	5.60	9.4
	1065	1/2	Air									
	760	16	Air									
29RS[c]	1065	2	Water	MT43	0.6×10^{20}	675	67.2	650	143,210	178,970	4.73	9.4
	1065	1/2	Air									
	760	16	Air									
26RS	1065	2	Water	MT43	1.1×10^{20}	675	67.2	26	141,550	181,130	13.00	12.5
	1175	1/2	Air									
	900	4	Air									
27RS	1065	2	Water	MT43	1.1×10^{20}	675	67.2	650	132,450	174,830	8.80	6.3
	1175	1/2	Air									
	900	4	Air									
31RS	1065	2	Water	MT43	0.9×10^{20}	675	67.2	650	129,960	165,560	7.47	11.0
	1175	1/2	Air									
	900	4	Air									
62RS	1065	2	Water	MT51	0.6×10^{20}	870	72.0	26	120,210	141,710	1.40	6.3
	1175	1/2	Air									
	900	4	Air									
63RS	1065	2	Water	MT51	0.6×10^{20}	860	72.0	870	47,270	52,970	2.60	15.4
	1175	1/2	Air									
	900	4	Air									
64RS	1065	2	Water	MT51	0.6×10^{20}	860	72.0	870	54,790	60,950	2.67	4.9
	1175	1/2	Air									
	900	4	Air									
71RS	1065	2	Water	MT51	0.6×10^{20}	870	72.0	650	125,410	165,060	4.27	6.3
	1175	1/2	Air									
	900	4	Air									
73RS	1065	2	Water	MT51	0.6×10^{20}	870	72.0	870	49,400	53,360	3.07	4.8
	1175	1/2	Air									
	900	4	Air									
55RS	1065	2	Water	MT51	0.6×10^{20}	800	72.0	870	63,360b	65,060b	3.40b	8.0b
	1175	1/2	Air									
	900	4	Air									
56RS	1065	2	Water	MT51	0.6×10^{20}	800	72.0	870	57,363b	58,210b	3.60b	9.6b
	1175	1/2	Air									
	900	4	Air									

TABLE 3.6 (Contd.)

RENE' 41 IRRADIATED SPECIMEN TENSILE TEST DATA
EXPERIMENTS 1, 2, AND 3

Specimen[a]	Pre-Irradiation Treatment			Capsule	Irradiation Conditions			Test Temperature, °C	0.2-Percent Yield, psi	Ultimate Strength, psi	Elongation, %	Reduction Of Area, %
	Temperature, °C	Time, hr	Quench/Cool		Dosage, nvt (En ≥ 1 Mev)	Temperature, °C	Time, hr					
76RS[c]	1065	2	Water	MT51	0.6×10^{20}	870	72.0	870	35,860	40,750	3.13	7.8
	1065	1/2	Air									
	760	16	Air									
79RS[c]	1065	2	Water	MT51	0.6×10^{20}	870	72.0	870	29,340	31,780	2.80	10.9
	1065	1/2	Air									
	760	16	Air									
Notched Specimens												
17RN[c]	1065	2	Water	MT43	0.4×10^{20}	675	67.2	650	-	203,730	-	-
	1065	1/2	Air									
	760	16	Air									
18RN[c]	1065	2	Water	MT43	0.4×10^{20}	675	67.2	650	-	198,840	-	-
	1065	1/2	Air									
	760	16	Air									
13RN	1065	2	Water	MT43	0.4×10^{20}	675	67.2	26	-	236,320	-	-
	1175	1/2	Air									
	900	4	Air									
14RN	1065	2	Water	MT43	0.4×10^{20}	675	67.2	26	-	236,320	-	-
	1175	1/2	Air									
	900	4	Air									
15RN	1065	2	Water	MT43	0.4×10^{20}	675	67.2	650	-	208,610	-	-
	1175	1/2	Air									
	900	4	Air									
19RN	1065	2	Water	MT51	0.6×10^{20}	870	72.0	870	-	77,420	-	-
	1175	1/2	Air									
	900	4	Air									
20RN	1065	2	Water	MT51	0.6×10^{20}	880	72.0	870	-	55,000	-	-
	1175	1/2	Air									
	900	4	Air									
21RN	1065	2	Water	MT51	0.6×10^{20}	870	72.0	870	-	66,500	-	-
	1175	1/2	Air									
	900	4	Air									

[a] All specimens from Heat TV-754.
[b] After irradiation, specimens 55RS and 56RS were heat treated at 1065°C for 2 hr and water quenched, plus 1175°C for 1/2 hr and air cooled, plus 900°C for 4 hr and air cooled.
[c] Specimens applicable to Experiment No. 3

TABLE 3.7

RENE' 41 IRRADIATED SPECIMEN TENSILE TEST DATA EXPERIMENTS NO. 1 AND 2

Specimen[a]	Capsule No.	Irradiation Conditions Dosage, ($E_n \geq 1$ Mev)	Temperature, °C	Time, hr	Test Temperature, °C	0.2-Percent Yield, psi	Ultimate Strength, psi	Elongation, %	Reduction Of Area, %
Smooth Specimens									
2R	MT27	0.7×10^{20}	550	96.0	26	111,650	132,340	6.70	19.7
3R	MT27	0.7×10^{20}	550	96.0	540	105,940	140,160	17.93	19.7
6R	MT38	0.5×10^{20}	675	71.3	26	94,530[b]	159,720[b]	21.93[b]	4.7[b]
10S	MT38	0.5×10^{20}	675	71.3	650	83,530[b]	124,840[b]	9.66[b]	13.9[b]
1R	MT27	0.7×10^{20}	550	96.0	26	111,500	134,000	-	-
4R	MT27	0.7×10^{20}	550	96.0	540	101,500	134,000	-	-
12S	MT38	0.5×10^{20}	675	71.3	26	121,000	139,000	-	-
8RS	MT38	0.5×10^{20}	675	71.3	650	105,000	140,500	-	-
10RS	MT38	0.5×10^{20}	675	71.3	650	107,000	135,000	-	-
Notched Specimens									
7RN	MT38	0.5×10^{20}	675	71.3	650	-	153,000	-	-
8RN	MT38	0.5×10^{20}	675	71.3	650	-	158,000	-	-

[a]All specimens from Heat TV-746 were heat treated, prior to irradiation, at 1065°C for 2 hr and water quenched, plus 1175°C for 2 hr and air cooled, plus 900°C for 4 hr and air cooled.

[b]After irradiation, specimens 6R and 10RS were heat treated at 1065°C for 2 hr and water quenched plus 1175°C for 1/2 hr and air cooled, plus 900°C for 4 hr and air cooled.

The ultimate tensile strengths of specimens from Heat TV-754 (Experiment No. 1), which received various thermal and irradiation treatments, are presented in Figure 3.7 as a function of test temperature. The irradiated specimens had approximately 10 percent lower strength than the corresponding control specimens, which received a simulated thermal history, at both irradiation temperatures of 650°C and 870°C. This 10 percent difference in the irradiated and control specimens appears to be constant at all tensile test temperatures. Both the 650°C control and irradiated specimens decrease in strength from room temperature to 650°C whereas the 870°C control and irradiated specimens increase in strength from room temperature to 650°C, then decrease in strength at 870°C.

The specimens from Heat TV-754 (Experiment No. 2), which were given a heat treatment after irradiation or simulated cycle show an increase in average strength, but are still within the same range as specimens that were not given a final heat treatment.

In Experiment No. 3, the specimens received a lower solution temperature treatment than the specimens given the standard heat treatment. At 650°C, the simulated cycle specimens (TV-754) have the same tensile strength as the specimens given the standard heat treatment. At the same temperature, 650°C, the irradiated specimens have higher strength than the specimens given the standard heat treatment (Experiment No. 1). At 870°C, however, the simulated and the irradiated specimens have lower strength than the corresponding specimens given the standard heat treatment.

The ultimate tensile strength of all notched specimens is greater than smooth specimens except at 870°C, where the value appears to be nearly the same. This would indicate the material is notch ductile but is approaching notch sensitivity at 870°C.

The yield strengths for the specimens (TV-754) used in Experiment No. 1 are presented in Figure 3.8. The specimens that were irradiated at 650°C have approximately 5 percent less yield strength at room temperature than the control specimens; at 650°C the yield strengths are nearly equal. The specimens irradiated at approximately 870°C have 10 percent less yield strength at room temperature and about 10 percent greater yield strength at the 650°C test temperature, than the control specimens. The 870°C yield strength data
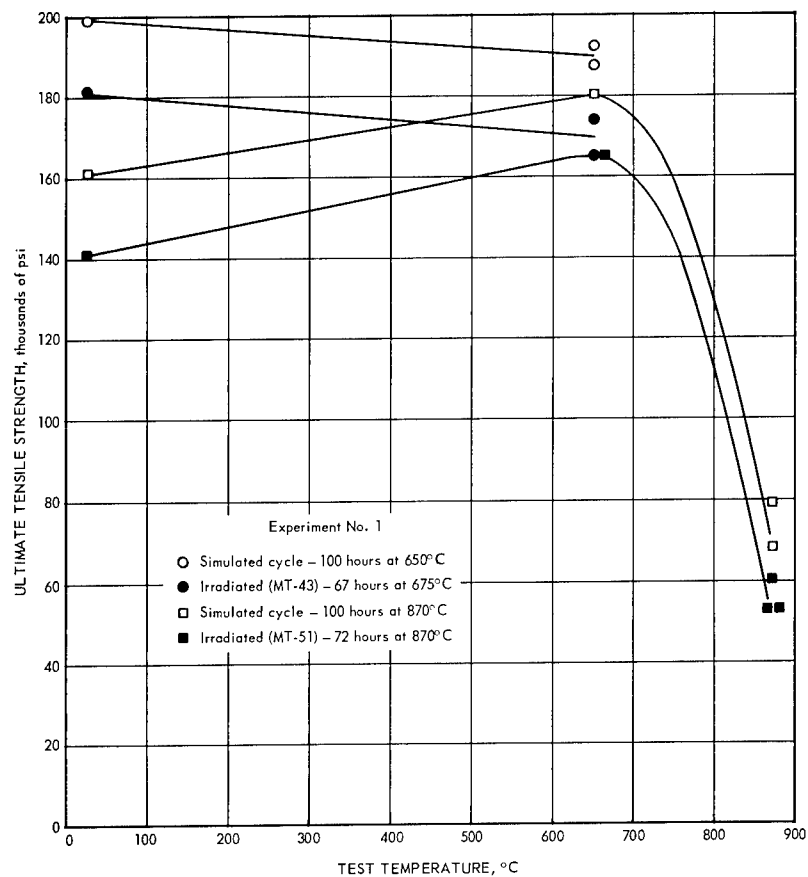
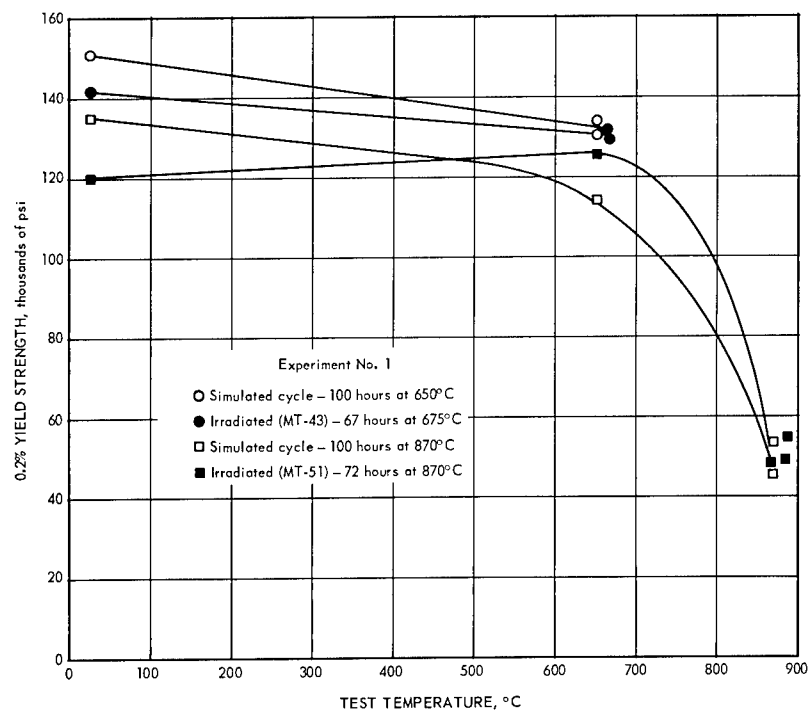Fig. 3.7 — Tensile strength of control and irradiated smooth Rene' 41
specimens — Heat TV-754

Fig. 3.8 — Yield strength of control and irradiated smooth Rene' 41
specimens — Heat TV-754

indicate very little effect is caused by irradiation when compared to the control data. The yield strength of irradiated specimens from Experiment No. 3, given the non-standard heat treatment, is much higher than the other specimens at irradiation and test temperatures of 650°C but much lower at irradiation and test temperatures of 870°C.

The percent of elongation for specimens (TV-754) versus test temperatures are shown in Figure 3.9. The marked decrease in ductility for specimens irradiated and tested at 870°C is apparent in the decrease in elongation (and also the reduction in area as listed in Tables 3.4 and 3.6) when compared to control specimens given a simulated cycle at 870°C. There also appears to be a similar trend for the specimens irradiated at 650°C.
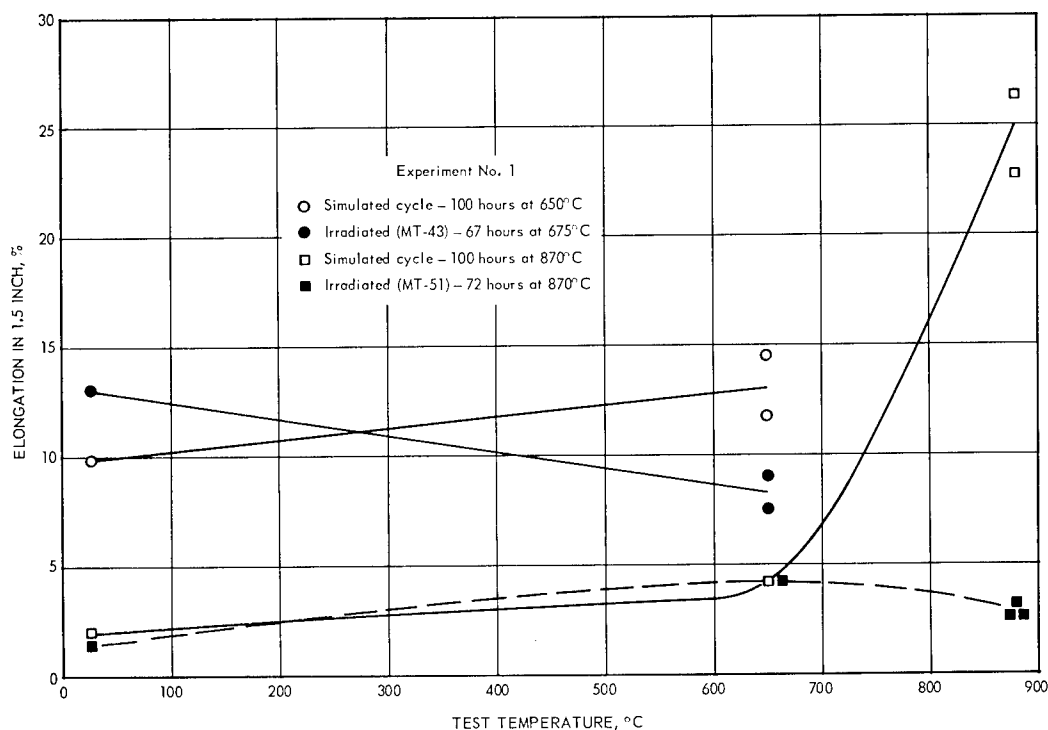

Fig. 3.9 — Elongation of control and irradiated smooth Rene' 41 specimens — Heat TV-754

The ultimate tensile strengths for the second heat (TV-746) of Rene' 41, indicate that at room temperature the specimens irradiated at 540°C have a lower tensile strength than the control specimens given a simulated temperature cycle. At a test temperature of 540°C, the irradiated specimens have a higher strength. This is not the case for the specimens irradiated at approximately 650°C; the data indicate that the irradiated specimens are stronger up to 540°C than the corresponding control specimens, but weaker at 650°C.

Specimens from Heat TV-746 (Experiment No. 2) irradiated at about 650°C, followed by post-irradiation heat treatment, had a higher tensile strength at room temperature but much lower tensile strength at 650°C; the control specimens given the simulated cycle followed by the standard heat treatment had about the same strength at 540°C but a little less strength at 650°C.

The irradiated and control notched specimens from Heat TV-746 also exhibited notch ductility in the temperature range from 26°C to 650°C when compared to the corresponding control data.

The irradiated specimens (TV-746) have a higher yield strength at both 540°C and 650°C except for the specimens that received the post-irradiation heat treatment (Experiment No. 2) which have a lower yield strength than the corresponding control specimens.

Creep-Rupture Results - Preliminary studies on the creep-rupture properties of Hastelloy X specimens were conducted at 650°C and 870°C. The deformation measurements were made by attaching a dial gage indicator to the upper load rod and also by using an Acotran LVDT transducer which recorded on a strip chart. Both indicators were in good agreement throughout the tests. Three irradiated specimens and three control specimens were tested. The first comparison was made at 650°C and 35,000 psi between a test specimen (32H) irradiated in MT-27 which received a post-irradiation heat treatment and a control specimen (139HS) which received only the standard heat treatment. The irradiated specimen ruptured in 244 hours and the control specimen in 278 hours. These rupture times are comparable to other corresponding test results at the same stress. The creep properties appear to be similar for the two specimens as shown in Figure 3.10.
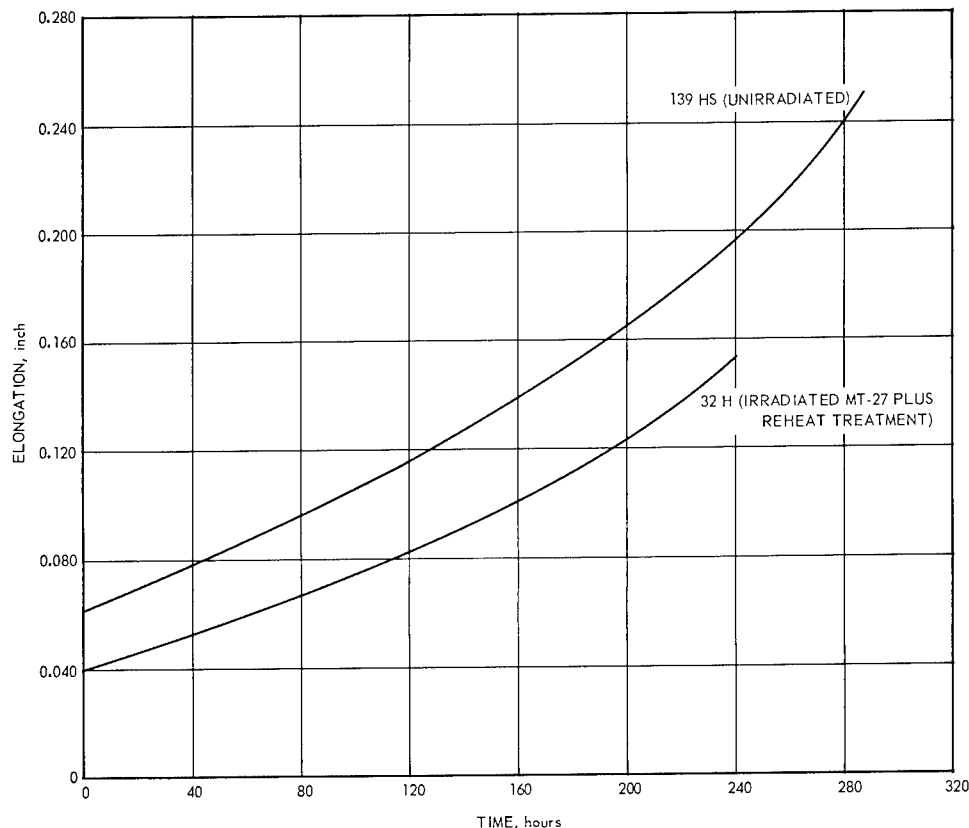

Fig. 3.10 – Creep of Hastelloy X at 650°C and 35,000 psi

Another comparison conducted at 650°C and 40,000 psi, was between three specimens, one specimen (34H), irradiated in MT-27 and thermally annealed at 650°C for 285 hours, and two control specimens, one as-machined (140HS) and the other receiving a simulated thermal cycle. The irradiated specimen ruptured at 126 hours, the as-machined control specimen at 130 hours, and the simulated specimen at 142 hours. Irradiated specimens that were tested at the same stress but did not receive the initial annealing treatment yielded an average rupture life of 32 hours. The creep curves for specimens 34H and 140HS are plotted in Figure 3.11. The irradiated specimen appears to have a constant
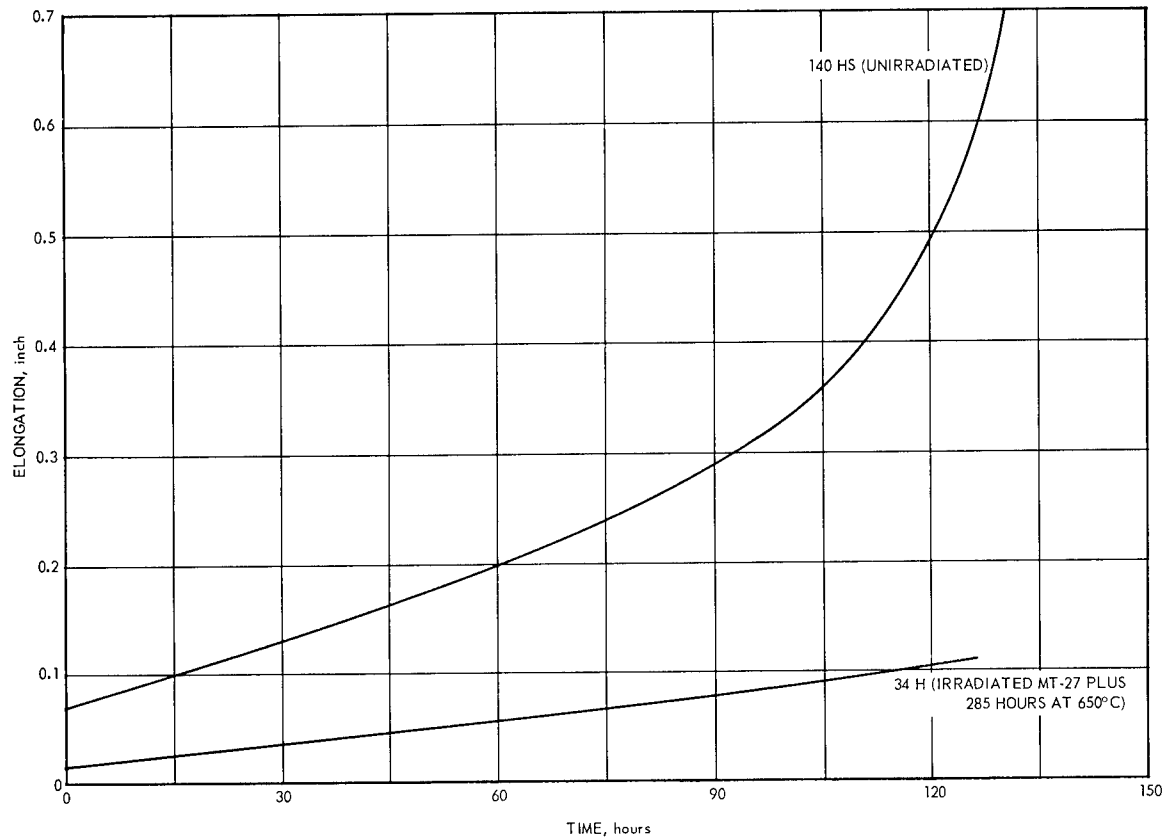
Fig. 3.11 — Creep of Hastelloy X at 650°C and 40,000 psi

creep rate up to the time of rupture. The control specimen, however, shows a large amount of third stage creep.

The deformation curves of Hastelloy X at 870°C are presented in Figure 3.12. In this investigation the irradiated specimen (40HS, MT-51) was thermally annealed at 870°C for 164 hours prior to testing at a stress of 10,000 psi. This specimen ruptured at 16.4 hours, whereas the unirradiated specimen ruptured at 50 hours. Two other irradiated specimens[*] tested at the same stress, ruptured at 14.6 and 26 hours. The steady state creep rate for the irradiated and control specimen appear similar. The control specimen exhibited about four times the total elongation of the irradiated specimen which is consistent with previously published data.[†]

STRUCTURE STUDIES

Metallographic examination is continuing on the A-286 samples[‡] that were irradiated specifically for structure studies. The samples were mounted and are currently being prepared for replication.

Electrolytic digestion studies of A-286 stress-rupture test specimens are continuing. To check further for an unidentified phase which was not observed in specimen 10AS[§] during its preliminary analysis but was observed in other A-286 specimens, a rediges-

---

[*]"High-Temperature Materials Program Progress Report No. 17, Part A," GE-NMPO, GEMP-17A, November 15, 1962, Figure 4.4, p. 34.
[†]Ibid., Table 4.5, p. 34.
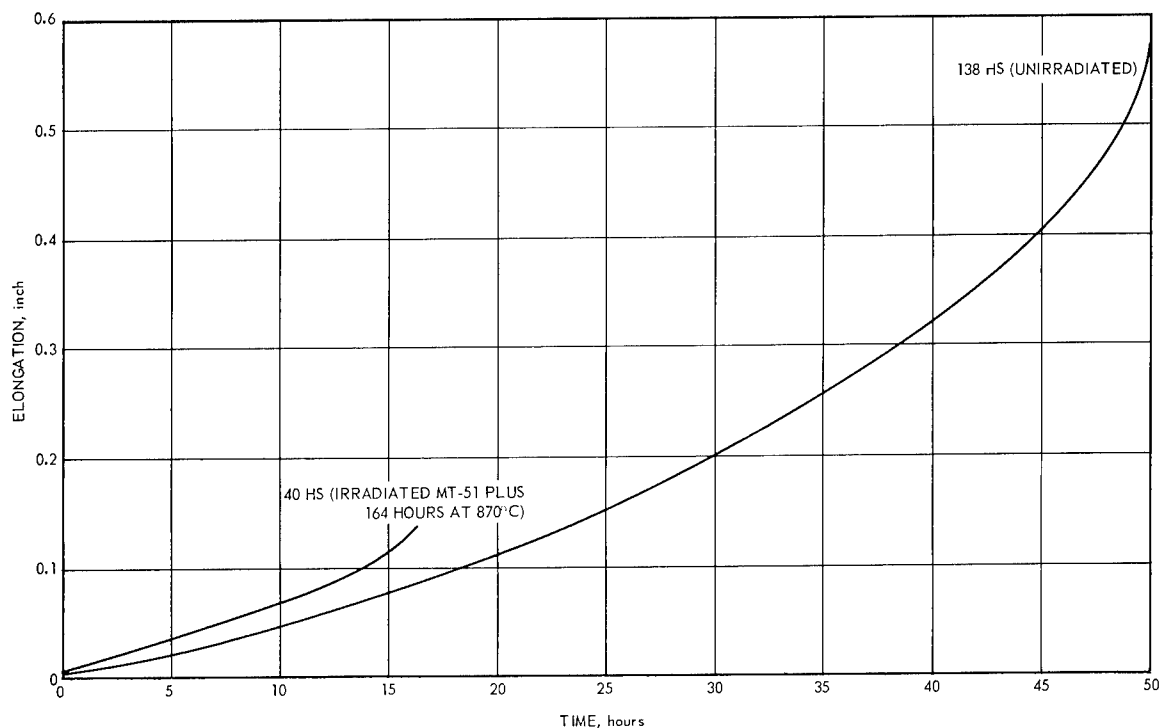[‡]Ibid., Table 4.13, p. 46.
[§]Ibid., p. 48.

Fig. 3.12—Creep of Hastelloy X at 870°C and 10,000 psi

tion of this specimen was performed. X-ray diffraction results of the second sampling (10AS-2) again showed only the TiC, Eta, and G phases, with the unidentified phase still not present. The main difference in the A-286 specimens (16K and 9AC) in which the unidentified phase was present was the irradiation temperature; specimens 16K and 9AC were irradiated at 540°C and specimen 10AS at 650°C.

Analysis of the unidentified phase from sample 16K indicates that the material may be face-centered cubic with a lattice parameter of about 10.3Å. These characteristics are similar to those for the carbide phase, $M_{23}C_6$, which is normally not present in A-286. $M_{23}C_6$ is a face-centered cubic structure and has a lattice parameter* of 10.6Å. Further evaluation will be required before the identity of this phase can be definitely established.

The results of X-ray fluorescence analysis obtained to date are summarized in Table 3.8. Samples 45AS and 16K are from Heat 2527 and samples B15649 and 10AS are from Heat 15649. Some of the data were corrected to a helium path since they were originally measured in an air medium.

Although there is some scatter in the analysis data, it appears that there is no appreciable difference between the concentration of the elements detected for the irradiated and the unirradiated material. Further analysis, however, are required to determine the concentration of carbon or other interstitial elements that were not detected by the X-ray fluoroscope. The results also indicate that the electrolytic digestion variables such as electric current density and acid concentration are not sensitive parameters with respect to the final residue obtained.

*Defense Metals Information Center Memorandum 160, Identification of Micro-constituents in Superalloys, November 15, 1962, p. 11.

TABLE 3.8

APPROXIMATE COMPOSITION OF RESIDUES FROM
DIGESTED A-286 SAMPLES

Sample	Elements[a]								
	Mo	Nb	Cu	Ni	Co	Fe	Mn	Cr	Ti
45AS-4[b]	0.7	–	1.6	2.3	–	4.2	–	1	8.8
45AS-4	0.7	–	3.7	2.0	–	4.2	0.2	1	5.4
45AS-1[b]	1.5	–	–	4.7	–	7.5	–	1	12.6
16K[b,c]	1.1	–	–	4.1	–	6.8	–	1	14.6
B15649-1A	0.9	0.3	5.3	6.2	0.1	6.1	0.2	1	7.0
B15649-1B	1.0	0.2	2.2	6.6	0.1	6.4	0.2	1	6.9
B15649-2A	1.4	0.3	2.1	9.3	0.2	7.6	0.2	1	10.1
10AS-2[c]	1.3	0.2	1.3	10.1	0.2	6.5	0.1	1	7.9

[a]Values obtained by X-ray fluorescence and arbitrarily normalized
to unity for Cr.
[b]Air path data corrected to equivalent helium path analysis.
[c]Irradiated sample material.

FUNDAMENTAL STUDIES

Iron Displacement Studies

A Monte Carlo* program written for the IBM 7090 computer was used to compute the number and energy spectra of primary knock-on atoms (PKA) produced in neutron-irradiated iron samples. Using this information, the number of displaced atoms was computed on the basis of the Kinchin-Pease displacement model. Neutron energy spectra for a test hole in the ETR reactor[†] was used to obtain typical results for irradiations in water-moderated reactors. Monoenergetic sources with energies in the range 10 to 10,000 Kev were used to study the energy dependence of the displaced atom population. Experimentally obtained angular distributions for neutron scattering were utilized to account for anisotropic neutron scattering in the center of the mass coordinate system. The effect of neutron slowing down in the irradiated sample and neutron leakage were automatically accounted for by the scattering angle and geometrical tracing routines, respectively, of the Monte Carlo program.

If one assumes the Kinchin-Pease model for atom displacements, the displaced atom density, d, in a monatomic sample is given by:

$$d = (Y/2\beta E_d) [I(O, E^*) + E^*(1-F^*)] \tag{1}$$

where

Y = number of PKA produced per incident neutron
E_d = displacement threshold energy
β = volume-to-surface ratio of the irradiated sample
E^* = ionization limit energy for PKA
F^* = fraction of all PKA ejected with energies below E^*.

The number of atom displacements, D, is equal to the product of β and d. $I(O, E^*)$ is the integral:

$$I(O, E^*) = \int_O^{E^*} Ef(E)dE \tag{2}$$

*J. R. Beeler and J. L. McGurn, "A Method for Computing Primary Knock-On Spectra in Polyatomic Material Irradiated by Neutrons," GE-NMPO, GEMP-101, October 1961.
[†]"High-Temperature Materials Program Progress Report No. 15, Part A," GE-NMPO, GEMP-15A, September 14, 1962, Figure 4.12, p. 53.

where f(e) is the normalized PKA differential energy spectrum. From the definitions of Y and β it follows that d is the number of displaced atoms per unit volume given one incident neutron per unit area of the column surface. Hence, for an isotropic neutron flux, ϕ, and an irradiation time, t, the total displaced atom production (TDP) would be:

$$TDP = d\phi t \qquad (3)$$

Following Wollenberger,[*] for example, it was assumed that PKA with energies less than E* lost energy solely by elastic collisions with other atoms, while PKA with energies above E* lost energy solely by ionization collisions and hence could not produce displaced atoms until they slowed down, below E*, into the elastic collision range.

In general, Y, I(O, E*), and F* are extensive quantities, i.e., they depend upon the size of the irradiated sample and the energy and angular distribution of the incident neutrons. In finite samples, both I(O, E*) and (1-F*) tend to increase as the neutron energy increases but Y tends to decrease with increasing neutron energy. In iron samples, this competition between opposing influences usually results in a plateua in d for neutron energies in the neighborhood of 1 Mev.

Iron Column - A plot of the atom displacements, D, in a small iron column (square base parallelepiped) is presented in Figure 3.13, as a function of neutron energy in the range 10 to 10,000 Kev. The length of the column was 6.35 cm and the base dimension was 0.2814 cm. An isotropic angular distribution for the neutron angle of incidence was used.

For this particular iron column $\beta = 0.069$. All iron samples are characterized by $E_d \simeq 25$ ev, $E* \simeq 56$ Kev, and F* = 1 for neutron energies below 800 Kev. The supplementary plots of Y, I(O, E*), and (1-F*) show how the variation of D with neutron energy evolves.

Semi-Infinite Medium - Neutron leakage tends to harden the PKA energy spectrum by truncating the neutron collision sequence in the high energy region. In general, leakage occurs by either neutron reflection or transmission. In a semi-infinite medium, which is irradiated by neutrons entering at its free surface, leakage is due solely to reflection, and, for this reason, the characteristics of PKA in a semi-infinite medium are of interest.

The number of displaced atoms, D, in a semi-infinite iron medium is plotted in Figure 3.14, as a function of neutron energy. Supplementary plots of I(O, E*), Y, and (1-F*) are also included to show how D evolves as the neutron energy increases.

Below 1 Mev, I(O, E*) is the principal factor in the displacement equation. Above 1 Mev, the sharp increase in (1-F*) and an increase in Y combine to maintain an increase in D in spite of the slow rise in I(O, E*) over this energy range.

Effect of Angular Distribution - If various combinations of the incident neutron angular distribution and the neutron scattering distribution are tried, a significant difference in PKA production is observed for a given neutron energy spectrum. The yield can be changed by a factor of 1.7, the number of displaced atoms by a factor of 1.6, and the average PKA energy by a factor of 1.3 by varying the source angular distribution and neutron scattering distribution. The number of displacements per PKA is relatively insensitive to these changes, however, having a maximum variation of about 10 percent.

A comparison of the atom displacement density for slabs and columns is presented in Figure 3.15. The results for isotropic neutron scattering are compared with those for

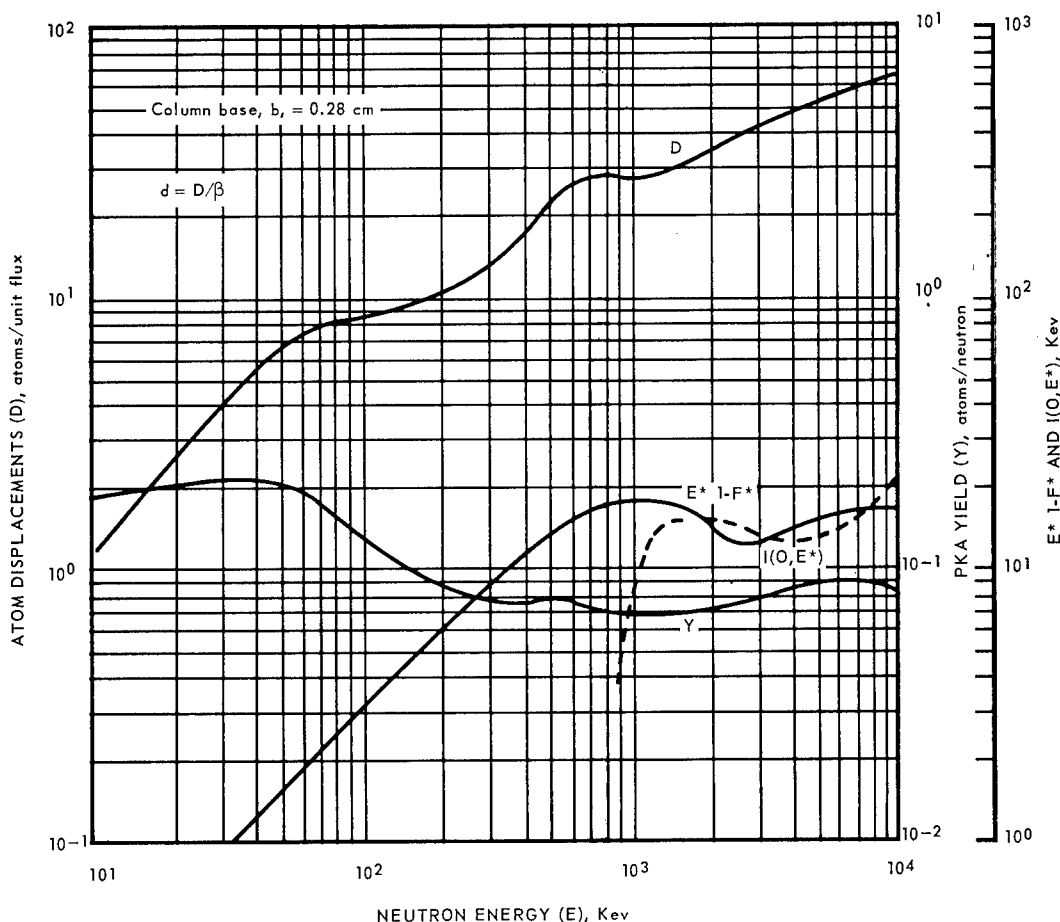[*] H. Wollenberger, Nukleonik, Vol. 4, 1962, p. 25.

Fig. 3.13 — Displacement parameters in a finite (0.28 by 0.28 by 6.35 cm) iron medium as a function of neutron energy from isotropic neutron source

anisotropic neutron scattering. Normally, incident neutrons with the ETR energy spectrum were used in these calculations. The displacement density is larger in columns with base b than in slabs with thickness t = b; the atom displacement density, d, for isotropic neutron scattering is about 1.5 times that for anisotropic neutron scattering.

CONCLUSIONS

Irradiation appears to affect underaged Rene' 41 test specimens more than overaged test specimens when irradiated and tested at a temperature of 650°C. The overaged specimen control and irradiated test data was within 5 percent of the corresponding data for specimens which received the standard heat treatment.

Overaged and underaged Rene' 41 test specimens that were irradiated and tested at 870°C did not show the pronounced difference noted at the lower test temperature.

Irradiation at 650°C and 870°C reduces the ultimate tensile strength of Rene' 41 by approximately 10 percent at all test temperatures. The tests indicate that Rene' 41 is notch ductile at the lower temperatures and approaches notch sensitivity at 870°C.

Elongation and reduction in area data for specimens irradiated at 870°C show ductilities comparable to those of the control specimens at all test temperatures except 870°C where there is a marked decrease.
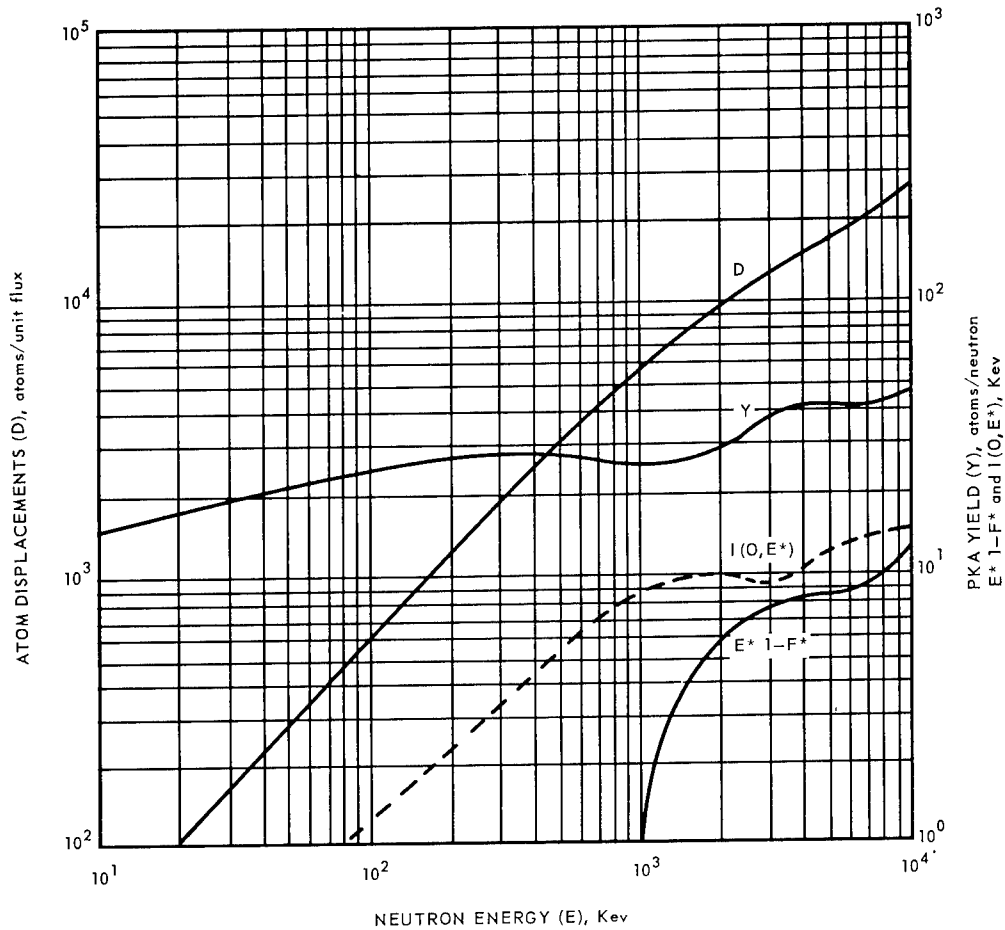
Fig. 3.14 — Displacement parameters in a semi-infinite iron medium as a function of neutron energy from an isotropic neutron source

Atom displacement production by primary knock-on atoms with energies greater than the ionization threshold energy was found by theoretical calculations to be enhanced in specimens of finite geometry relative to the displacements in the semi-infinite systems. The atom displacements will also depend on the angular distribution of neutrons incident on the material and also on the angular dependence of scattering within the medium.

The correlation of radiation effects, based on atom displacements, of in-reactor specimen tests of small dimensions with the corresponding effects in reactor pressure vessels of large dimensions will depend significantly on the material geometry and the angular distribution of the incident neutrons in addition to the neutron spectrum.

WORK PLANNED FOR NEXT PERIOD

The preliminary program on refractory metals will be continued with the creep-rupture testing of irradiated tungsten and molybdenum flat specimens. Refractory metal specimen fabrication and specimen irradiation will continue. Furnace operation and testing techniques will be established for handling radioactive test specimens.

Stress-strain diagrams of the irradiated and control tensile data will be evaluated in more detail to further interpret the effects of irradiation on the tensile properties of A-286, Rene' 41, and Hastelloy X.
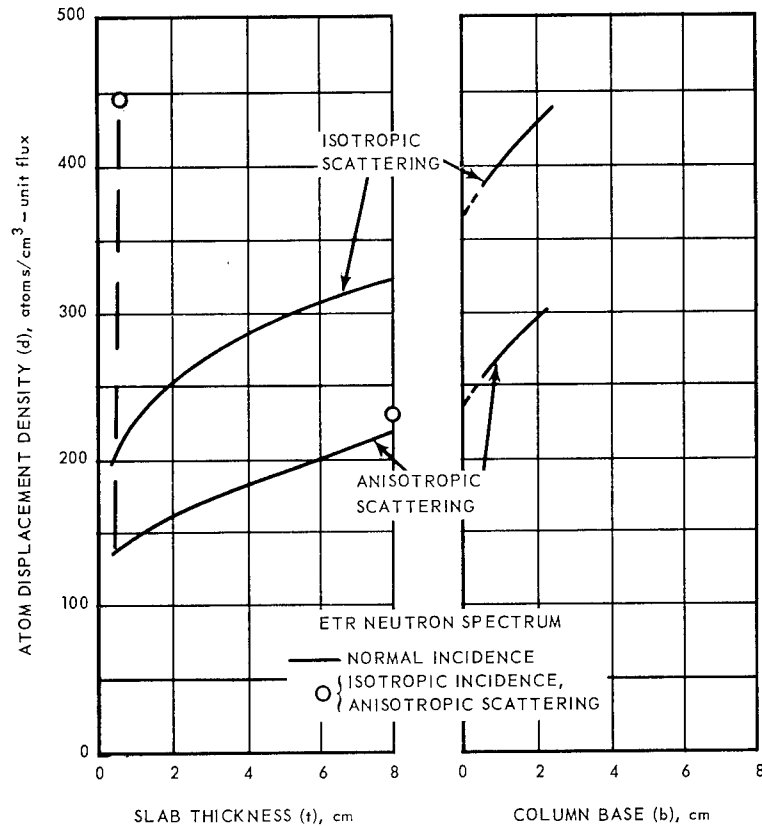
Fig. 3.15 — Atom displacement density for slab and column geometry

Work will continue on the theoretical predictions of atom displacements and the rate of anneal for various times and temperatures. Studies on a preliminary physical model to explain the changes in stress-rupture properties caused by neutron irradiation will continue.

Structure and fracture studies will continue with major emphasis on the A-286 alloy. Digestion techniques for separating the precipitates from the matrix will be continued with special attention to determining whether an unknown phase is formed due to the irradiation.

4. LONG TERM IRRADIATION TEST
OF 80Ni-20Cr FUEL ELEMENT SPECIMEN

(57301)

The objective of this task is to establish, on a preliminary basis, the stability of 80Ni - 20Cr fuel ribbon at elevated temperatures in air when subjected to neutron irradiation for long periods of time corresponding to burn-up levels of 25 percent of the U^{235} atoms present.

No further work was done during this reporting period. A final summary will be included in the 1963 High-Temperature Materials Annual Report.

5. APPENDIX

The "High-Temperature Materials Program Progress Reports" previously issued in this series are listed below. The first two reports were each issued as one document, containing both the classified and unclassified portion. The subsequent reports were issued as two documents; part A, the unclassified portion and part B, the classified portion.

Report No.	Report Period	Publication Date
NMP-HTMP-1	May 1961 - June 30, 1961	July 15, 1961
GEMP-2	July 1, 1961 - July 31, 1961	August 15, 1961
GEMP-3, A and B	July 1, 1961 - August 31, 1961	September 15, 1961
GEMP-4, A and B	August 1, 1961 - September 30, 1961	October 15, 1961
GEMP-5, A and B	August 15, 1961 - October 15, 1961	November 15, 1961
GEMP-6, A and B	September 15, 1961 - November 15, 1961	December 15, 1961
GEMP-7, A and B	October 15, 1961 - December 15, 1961	January 15, 1962
GEMP-106, A and B (First Annual Report)	Calendar Year 1961	February 28, 1962
GEMP-9, A and B	January 1, 1962 - February 15, 1962	March 30, 1962
GEMP-10, A and B	January 1, 1962 - March 15, 1962	April 16, 1962
GEMP-11, A and B	February 15, 1962 - April 15, 1962	May 15, 1962
GEMP-12, A and B	March 15, 1962 - May 15, 1962	June 15, 1962
GEMP-13, A and B	April 15, 1962 - June 15, 1962	July 31, 1962
GEMP-14, A and B	May 15, 1962 - July 15, 1962	August 15, 1962
GEMP-15, A and B	June 15, 1962 - August 15, 1962	September 14, 1962
GEMP-16, A and B	July 15, 1962 - September 15, 1962	October 15, 1962
GEMP-17, A and B	August 15, 1962 - October 15, 1962	November 15, 1962
GEMP-18, A and B	September 15, 1962 - November 15, 1962	December 14, 1962